Use of Polyesters in Fused Deposition Modeling for Biomedical Applications

Macromolecular Bioscience
www.mbs-journal.de

Use of Polyesters in Fused Deposition Modeling for Biomedical Applications

Arianna Grivet-Brancot, Monica Boffito, and Gianluca Ciardelli**

In recent years, 3D printing techniques experience a growing interest in several sectors, including the biomedical one. Their main advantage resides in the possibility to obtain complex and personalized structures in a cost-effective way impossible to achieve with traditional production methods. This is especially true for fused deposition modeling (FDM), one of the most diffused 3D printing methods. The easy customization of the final products' geometry, composition, and physicochemical properties is particularly interesting for the increasingly personalized approach adopted in modern medicine. Thermoplastic polymers are the preferred choice for FDM applications, and a wide selection of biocompatible and biodegradable materials is available to this aim. Moreover, these polymers can also be easily modified before and after printing to better suit the body environment and the mechanical properties of biological tissues. This review focuses on the use of thermoplastic aliphatic polyesters for FDM applications in the biomedical field. In detail, the use of poly(ϵ-caprolactone), poly(lactic acid), poly(lactic-*co*-glycolic acid), poly(hydroxyalkanoate)s, thermoplastic poly(ester urethane)s, and their blends is thoroughly surveyed, with particular attention to their main features, applicability, and workability. The state-of-the-art is presented and current challenges in integrating the additive manufacturing technology in the medical practice are discussed.

1. Introduction

In the last decades, 3D printing has gained an ever-growing importance in different manufacturing sectors, including the biomedical one. This increasing interest is mainly due to the improvement in the basic processes underpinning the different printing techniques and the development of new printable materials.[1] The main advantage of 3D printing, also known as additive manufacturing or rapid prototyping, lies in the possibility to obtain highly complex designs that would be extremely difficult to achieve using conventional methods, such as molding or forming. Moreover, it allows for a high customization of the products in a cost-effective manner,[2] which is especially important toward patient-specific applications in the medical field. For instance, according to this approach, prostheses or bone replacements can be directly modeled based on each singular defect, starting from images obtained via different kinds of medical imaging techniques, such as magnetic resonance imaging or computed tomography (CT).[3]

A typical 3D printing process starts from a computer-aided design (CAD) model. In order to guide the machine through a layer-by-layer manufacturing process, the model needs to be divided into suitably thick slices through a slicer software which generates a G-code then transferred to the printer to realize the final object. A schematic representation of this process is reported in **Figure 1**. Some postprocessing is applied in some cases for the final realization of the construct and improve its mechanical properties.[4] In the biomedical field surface polishing can be exploited to modulate construct roughness, with relevant implications on cell behavior, as recently surveyed by Cai et al.[5] The standard classification of 3D bioprinting identifies seven different categories of market-available techniques: material extrusion, powder bed fusion, binder jetting, sheet lamination, material jetting, vat photo polymerization, and directed energy deposition.[6,7]

Material extrusion techniques are particularly suitable for polymeric materials, which are currently used in more than half of the additive manufacturing applications.[8] Fused deposition modeling (FDM) is the most popular among these methods, with more than a hundred producers and distributors present on the market.[9] FDM, which is also known as fused filament fabrication (FFF), was developed in the late 1980s and marketed starting from the 1990s by Stratasys Inc.[10] The technique consists in the deposition of layers obtained by polymers heated slightly above their melting temperature and extruded through a nozzle, following a software-controlled path (**Figure 2**).[11] It is considered a

A. Grivet-Brancot, M. Boffito, G. Ciardelli
Department of Mechanical and Aerospace Engineering
Politecnico di Torino
Corso Duca degli Abruzzi, 24, Torino 10129, Italy
E-mail: monica.boffito@polito.it; gianluca.ciardelli@polito.it
A. Grivet-Brancot
Department of Surgical Sciences
Università di Torino
Corso Dogliotti 14, Torino 10126, Italy

The ORCID identification number(s) for the author(s) of this article can be found under https://doi.org/10.1002/mabi.202200039

DOI: 10.1002/mabi.202200039

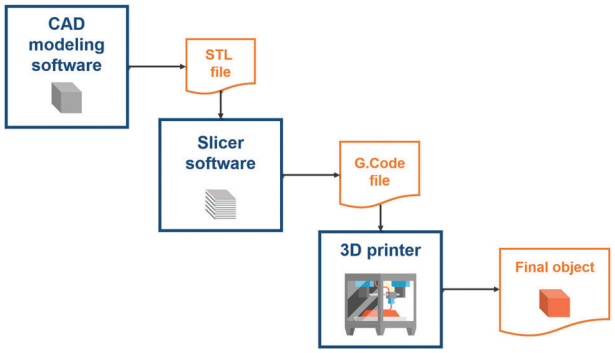

Figure 1. Schematic representation of a general 3D printing process, from virtual modeling to the final object.

low cost method with a manufacturing time comparable to other printing techniques, such as stereolithography.[12,13]

Thermoplastic polymers are the preferred materials for this application; the relatively low melting temperature of many of them allows for a safe and easy use also in office-like environments.[4] Ready-to-use filaments based on these polymers as such or additivated with particles, fibers or functional excipients (e.g., plasticizers) are available on the market; however, it is also possible to process custom-made material pellets to obtain filaments then 3D printed or to directly print the final object.[14] Moreover, multiple heads can be combined within the same printer to simultaneously extrude materials with different properties.[15–17]

Acrylonitrile butadiene styrene (ABS) and poly(lactic acid) (PLA) are the most diffused materials to produce filaments for FDM.[9,18] ABS is not suitable for tissue engineering applications because it is not biodegradable and, in medical applications, can only be used for surgical planning models.[19,20] However, not only PLA but polyesters in general are used in the biomedical field in a wide range of applications, because of their biocompatibility, biodegradability, and lack of toxicity.[21] Aliphatic polyesters, as the above-mentioned PLA and its copolymer with glycolic acid, poly(lactic-*co*-glycolic acid) (PLGA), poly(ϵ-caprolactone) (PCL), and poly(hydroxyalkanoate)s (PHA)s have been commonly employed in FDM. Other interesting materials for FDM processing are poly(ester urethane)s (PUs), due to their high chemical versatility which can be exploited to synthesize a wide plethora of polymers matching the requirements of many different applications. **Table 1** resumes the chemical structures and abbreviations of these polymers. Scaffold productions for tissue engineering[22,23] and organ reconstruction,[24,25] bone regeneration,[26–28] and drug delivery systems[29,30] are among the most targeted applications. As for most of the 3D printing techniques, FDM permits a fine control on the geometrical features of the printed constructs, such as filament orientation, pore size, and general scaffold structure.[31] The possibility to insert biological cues through dip-coating or surface-functionalization procedures is widely exploited to improve the biomimicry and biocompatibility of 3D printed constructs. Additionally, according to a recently developed strategy, 3D bioprinting, and FDM can also be integrated into one single device, leading to the direct 3D bioprinting of a bioink (i.e., a cell containing materials ink) into each FDM-printed layer.[21]

This review has been conceived within this context and aims to provide readers with an up-to-date critical analysis on the processing of aliphatic thermoplastic polyesters with FDM and their applications in the biomedical field. After introducing the requirements of polymeric materials in FDM applications, attention has been focused on papers published over the last decade. Research works on PCL, PLA, PLGA, PHAs, and PUs will be thoroughly investigated, also considering their composites, copolymers, and blends. Additionally, a discussion on the present achievements and future perspectives will be provided.

1.1. Key Material Requirements and Parameters in Biomedical FDM Applications

The selection of suitable materials and the optimization of process parameters are the most important factors in FDM

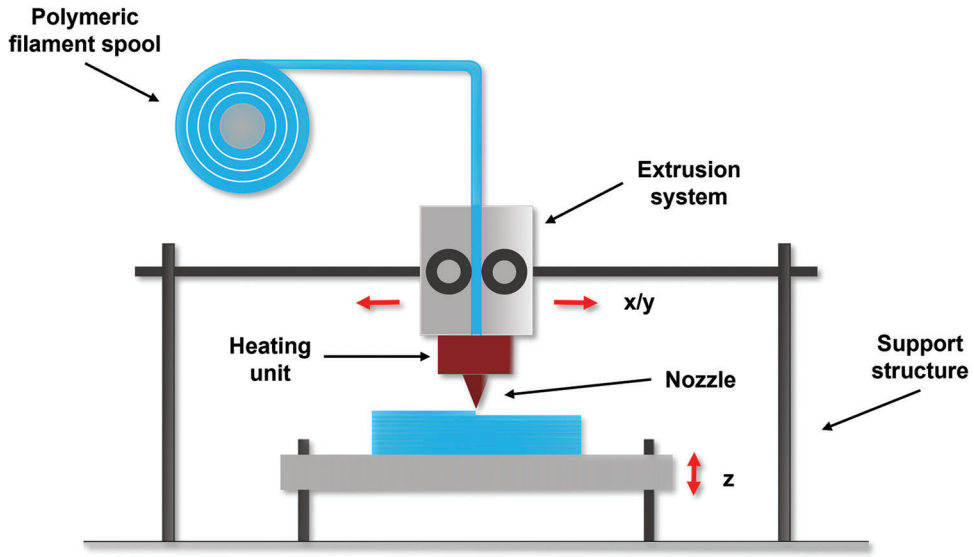

Figure 2. General representation of an FDM machine.

Table 1. Chemical structures and abbreviations of polyesters commonly used in FDM applications.

Polymer name	Abbreviation	General chemical structure
Poly(*ϵ*-caprolactone)	PCL	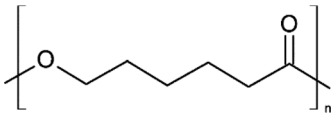
Poly(lactic acid)	PLA	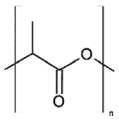
Poly(lactic-*co*-glycolic acid)	PLGA	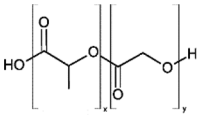
Poly(hydroxyalkanoate)s	PHAs	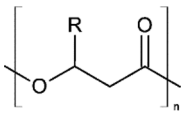
Poly(ester urethane)s	PUs	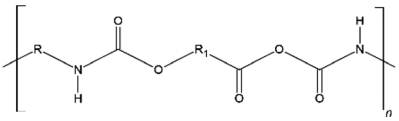

applications, and they are especially important in the medical field due to the strict requirements that biomedical devices should fulfill. As the literature reports several studies dedicated to this subject,[4,9,32–36] only a brief recap of the most relevant issues and requirements will be provided in this work.

Several parameters need to be adjusted for printing quality and mechanical properties of the final part to be optimal, both for biomedical and general industry purposes. The definition of design and machine parameters is usually the main focus of the printing optimization process. The build orientation of the part, the thickness of each deposited layer, the raster angle relative to the *x*-axis of the bed and the infill pattern used to build each layer are among the most studied characteristics. Their effect on the resulting part mechanical properties has been extensively investigated,[35,37,38] and an influence on the elastic properties has been evidenced.[4] It has indeed been reported that the compressive strength is influenced by the raster angle, while on the other hand tensile strength is affected by layer thickness.[39] However, for tissue engineering scaffold production some additional considerations are needed. For example, the presence of high porosity and interconnected channels, which is generally considered detrimental for additive manufacturing parts, is crucial to ensure gas and nutrient exchange and support cell proliferation inside the struct.[40] Moreover, it has been suggested that the infill pattern should be adjusted to provide a minimum pore size of 100 μm, that should be raised to at least 200 μm for bone tissue applications, to result in proper regeneration and vascularization.[41]

Nevertheless, it should be kept in mind that the parameters mentioned until now are all strongly related to the properties of the feeding materials used, so their optimization should be always correlated with the polymer characteristics. First, FDM materials should have good melt viscosity properties[41] and their printing should be performed at shear rates at which they show a shear thinning behavior.[42] As also mentioned before, thermoplastic polymers usually present this characteristics at least to some extent and are therefore among the ideal candidates for FDM applications. Printing temperature, which is another crucial factor, can be varied in order to maximize these rheological performances. Yet, the effect of longer times at high temperatures on the polymer physicochemical properties should be thoroughly considered. Semicrystalline polymers show a greater resistance to elevated temperatures than amorphous ones and are generally able to better preserve their mechanical properties.[9] Still, the presence of crystallites can hinder the mobility of the polymeric chains during solidification and the change in volume following crystallization can result in shrinkage, warping, and delamination of the final produced part.[38,42,43] The binding between subsequent layers is also related to these characteristics and is the key factor affecting the anisotropy of FDM printed parts in the building direction.[37,44] Printing temperature plays an important role in this case, since strong bonds between layers can form only if the newly deposited material stays above its glass temperature (T_g) for a sufficient time,[43] but as already mentioned the polymer thermal stability must be always taken into account. Especially in the tissue engineering field, possible degradation of the materials upon the heating and shear stress experienced during the production process could be critical if toxic debris and degradation products are released after implantation.

The prediction of the final part quality and characteristics is a multifaceted issue, involving many interconnected factors

that need to be finely tuned and balanced to achieve the optimal result. As explained, the feeding materials are highly stressed by different phenomena such as heat transfer, fluid flow and solidification in different stages, and adhesion between layers. Numerical models that aim to predict the best parameters by combining finite element analysis with thermal simulations have been proposed,[35,45] although with few specific studies in the biomedical framework.[28,46] However, a deeper investigation of material rheological properties and thermal response should be performed, in particular when additives, plasticizers or fillers are added as is common for biomaterial processing. In this sense, as also noted elsewhere, the simple evaluation of the melt flow index is not sufficient to understand the complex response to the various stimuli imparted to the material in the entire printing process.[47]

Many of the questions presented in this paragraph will be discussed in more detail in the following sections, referring to the specific material and application considered.

2. Poly(ϵ-caprolactone)

PCL is one of the most diffused thermoplastic polyesters used in the biomedical field. It can be obtained by different polymerization methods, all based on the ring-opening of ϵ-caprolactone monomers,[48,49] and using different catalysts, e.g., stannous octoate.[50] At physiological temperature, PCL is semicrystalline with low tensile strength and high elasticity, due to the presence of amorphous regions.[51] It possesses a very low glass transition temperature (T_g) of −60 °C and a relatively low melting temperature (T_m) around 60 °C.[52] PCL is also commercially available in the medical grade[53,54] and generally considered biocompatible and biodegradable; however, it can take up to 2–3 years for the polymer to completely degrade,[55,56] which is longer compared to other commonly used polyesters like PLGA (from several weeks to months).[57] This behavior can be correlated in PCL with the presence of a limited number of ester bonds that can be enzymatically hydrolyzed once implanted.[51] For this reason, this polymer is preferred for long-term applications and scaffolds for hard tissue replacement (e.g., bone tissue), that require good mechanical properties and a prolonged stability over time to allow a complete tissue regeneration.[58,59]

2.1. Scaffold Parameter Optimization

Many studies have been conducted to determine the suitability of PCL for the creation of scaffolds for tissue engineering applications by FDM. The mechanical properties of printed PCL scaffolds have been extensively evaluated. For instance, Hutmacher et al.[60] demonstrated that honeycomb-like PCL scaffolds exhibited a compression strength comparable to that of hard tissues (compressive stiffness in wet conditions between 20 and 30 MPa, depending on layer geometry) and retained their mechanical properties in a physiologically simulated ambient for 5–6 months, allowing tissue colonization. Similarly, Zein et al.[54] designed different scaffold architectures with anisotropic mechanical properties, which could be properly tailored to match different types of tissues by changing the filament orientation and construct porosity. Importantly, this study also demonstrated that PCL is not significantly degraded by the melting process used to obtain the polymeric filament. This aspect is particularly relevant for melting extrusion techniques and has been underlined also in other works,[54,61] although in many cases only the final structure properties are taken into account, without comparing them to the characteristics of the bulk material.

The compatibility of the scaffolds with different types of cells, such as fibroblasts[60] and cardiomyoblasts[62] has been widely evaluated in the literature, demonstrating their ability to sustain the cell growth up to several weeks. Cell response was also found to be highly dependent over the printing parameters (filament thickness, infill density).[60,62] Neovascularization in tissue substitutes is one of the crucial and still critical aspects to consider during scaffold design. Indeed, in the absence of angiogenesis only small structures can be adequately perfused, thus sustaining cell growth and proliferation. Muller et al.[63] developed a microstructured pattern inside a PCL scaffold using FDM to mimic a native capillary system. The authors demonstrated that new vasculature formed inside the channels 3 weeks post subcutaneous implantation of scaffolds seeded with porcine bone-marrow-derived mesenchymal stem cells (MSCs) into a rat model.

Despite the general good properties of PCL, many groups focused on the use of fillers, both organic and inorganic, to create PCL-based composites or blends and achieve better mechanical properties or a greater biocompatibility.[59] Regarding the use of inorganic additives, Korpela et al.[61] demonstrated that adding nanometric bioactive glass particles to PCL leads to an increase around 30–40% in strength, stiffness and compressive strength. However, filler addition increased the viscosity of the melt, making the printing process more difficult, with layers showing a not perfect adherence (**Figure 3**A).[61] Organic additives have also been used, as the relatively low melting temperature of PCL allows for their simultaneous processing.[64] Polysaccharides are interesting candidates in this sense and they have been utilized in combination with PCL also with other rapid prototyping techniques.[65] Recently, Zhao et al. used different percentages of starch (between 1 and 11 g every 100 g of PCL) to improve the crystallinity and the solidification rate of the final printed structures. Moreover, the printing temperature between 80 and 90 °C allowed the additional incorporation of bioactive agents (i.e., quaternary ammonium-73 and poly(hexamethylene biguanidine)) for antibacterial purposes.[64]

The low T_m of PCL is an interesting asset in view of its use as structure forming material in FDM processes. Indeed, this feature permits to combine this polymer with 3D printed hydrogels or bioinks and to protect thermally labile structures and materials. Kang et al.[66] used PCL as support material to produce 3D printed organs, by simultaneously printing the thermoplastic polymer with cell-laden and cross-linkable hydrogels based on natural polymers (i.e., a mixture of gelatin, fibrinogen, hyaluronic acid, and glycerol). PCL filaments were used either in the external part to give mechanical strength to the entire structure or to form microchannels inside the organ to provide nutrient and oxygen to the cells present in the inner parts of the constructs, sensibly improving survival, and functionality.[66] In another study, microspheres formed by PLA and decellularized extracellular matrix (DM) were dispersed in a PCL matrix and then extruded into filaments for FDM.[67] The combination of the PLA shell and the

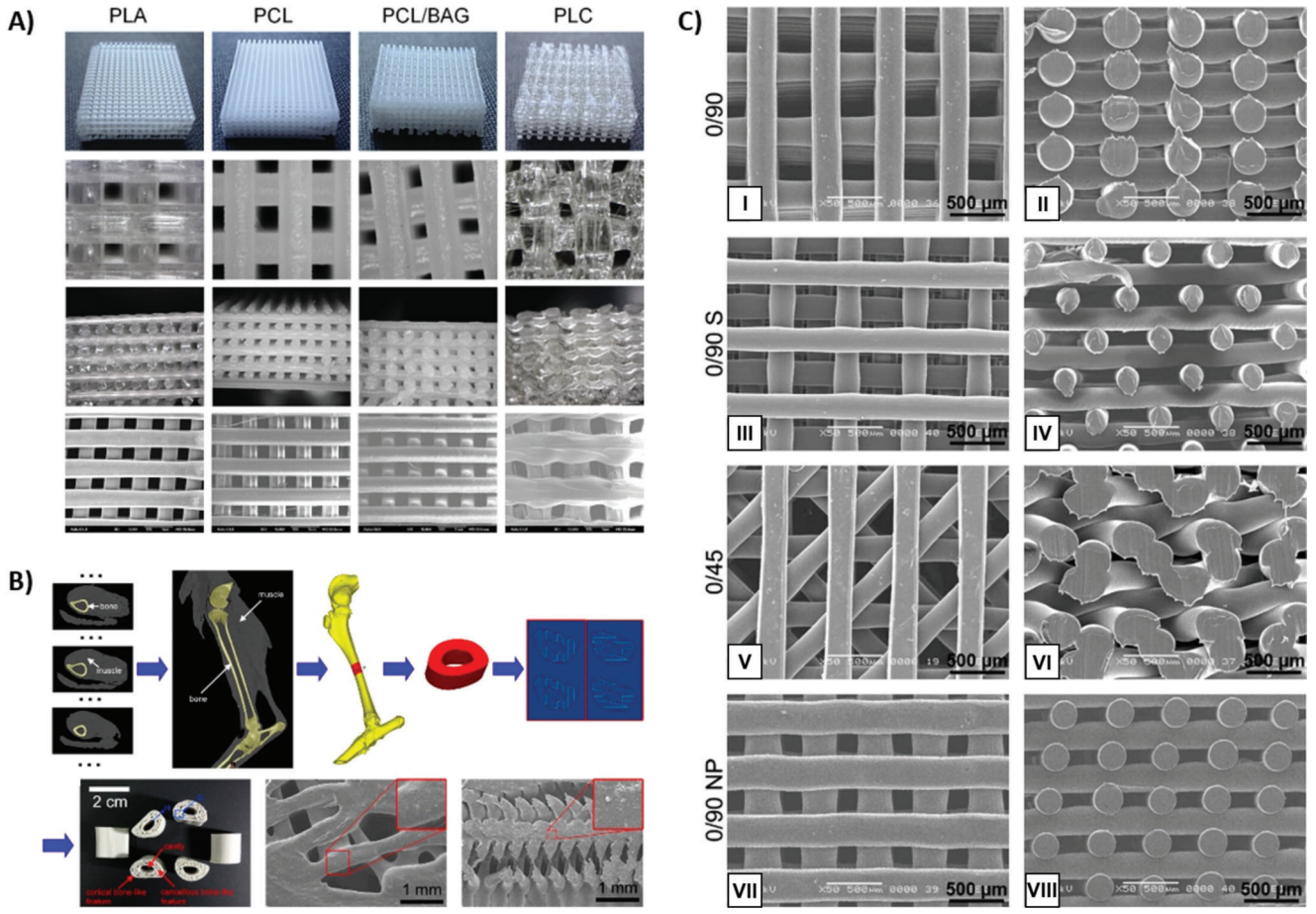

Figure 3. Example of scaffolds obtained through FDM. A) Images of FDM structures made of different polymers: PLA, PCL, PCL and bioglass composite (PCL/BAG), and PLA/PCL copolymer (PLC). Reproduced with permission.[61] Copyright 2013, Wiley Periodicals LLC., Inc. B) Schematic representation and Scanning Electron Microscope (SEM) images of an artificial bone substitute obtained by printing PCL and hydroxyapatite (HA). Adapted with permission.[85] Copyright 2013, Elsevier. C) SEM images of PCL scaffolds with different pore orientation: 0/90 (I-II), 0/90 S (shifted between layers, III–IV), 0/45 (V–VI), 0/90 NP (narrow pores, VII–VIII). Adapted with permission.[71] Copyright 2014, American Chemical Society.

mild printing temperature (65–70 °C) of PCL preserved the native conformation and bioactivity of the DM.

2.2. Bone Tissue Engineering Applications

Hard tissues, especially bone, are one of the most addressed targets for FDM applications with PCL. This preference is, as previously highlighted, mainly due to the mechanical characteristics obtained by processing this polymer. It is indeed possible to create scaffolds, which degradation rate is compatible with the regeneration of complex tissues, while maintaining the required stability. However, pore architecture and surface modification must be finely combined and optimized to achieve a good cell response and promote bone regeneration.[68,69] The reason resides on the native hydrophobicity of PCL, which requires some functionalization procedures (e.g., surface coating, blending with natural polymers) to create a more attractive environment for cell colonization. Pore size, interconnection and geometry, on the other hand, are important to provide the correct nutrient and oxygen exchange, thus allowing cell infiltration in the internal part of the scaffold.[70–72] In this sense, Declercq et al.[71] printed scaffolds with different pore orientations (Figure 3C) and performed different types of surface modification. They found that bioactive coatings, such as gelatin immobilization and fibronectin absorption, lead to better results than non-bioactive oxygen plasma treatment. Furthermore, filament orientation and the subsequent porosity influenced cell spreading and survival, with better results for the 0°/45° printing orientation (60–80% of porosity) compared to the 0°/90° lay-down pattern. Similar results were reported by Yilgor et al.,[72] who correlated the improved cell proliferation and colonization to the larger surface area available in the more compact designs. They also performed in vivo studies loading PLGA/poly(3-hydroxybutyrate-*co*-3-hydroxyvalerate) (PHBV) particles containing osteogenic growth factors (i.e., bone morphogenetic proteins (BMPs) 2 and 7) into PCL printed scaffolds, demonstrating the ability of the combined system to regenerate large bone defects.[72] Another study was performed by Chen et al.,[73] in which PCL scaffolds with ellipsoidal pores (semiaxes 120 and 170 μm) were filled with self-assembling extracellular matrix (ECM) components (i.e., hyaluronic acid, collagen) after production and cultured both in static and dynamic conditions.

Although better cell compatibility was found also for native PCL 3D printed constructs compared to results obtained with PCL porous matrices obtained through the conventional salt leaching technique, ECM-modified scaffolds provided better cell dispersion and differentiation in the deeper regions of the structures under optimized dynamic cell culture.[73] In another study, Li et al.[74] coated FDM-printed PCL scaffolds through immersion in platelet rich plasma (PRP) followed by freeze-drying, demonstrating the efficacy of the resulting hybrid matrices in promoting mineralization and osteogenesis in a rat calvarial defect after 12 weeks of implantation.

In the previously discussed studies, pore size was generally comprised between 100 and 600 μm, which is considered the best interval for in vivo bone ingrowth.[72,75] However, Temple et al.[76] successfully developed PCL scaffolds with larger pores (around 800 μm), to allow the culture of human adipose-derived stem cells (hADSCs) aggregates. The aim in this case was to induce hADSC differentiation toward both the osteogenic and vascular lineages, thus leading to the formation of new vascularized bone.[76,77]

A common strategy to improve the osteogenic properties of PCL is the use of calcium phosphate mineral additives.[26,78,79] One of the most diffused is β-tricalcium phosphate (β-TCP), due to its similarity with the mineral phase of natural bone. Bruyas et al.[80] systematically characterized the effects of the incorporation of different quantities of β-TCP into PCL FDM-printed scaffolds. The authors highlighted that an increasing amount of β-TCP (up to 60% w/w) leads to a faster degradation in accelerated conditions (i.e., in 5 M NaOH solution), from <1% for pure PCL to complete degradation for 60% β-TCP-loaded PCL samples after 54 h incubation. Moreover, an increase in stiffness and loss of elasticity was also observed when the additive content was raised; however, for highly porous constructs no significant differences in mechanical properties were observed comparing native and composite scaffolds.[80] A similar behavior was evidenced by another group[81] that compared a commercial product (Osteopore, Singapore, PCL-20% β-TCP) to a custom-made scaffold formed by PCL and 20% w/w biphasic calcium phosphate (BCP), which is composed by hydroxyapatite and β-TCP. More in detail, the commercial product was an FDM-fabricated matrix, while the newly designed scaffold was obtained through a melt stretching and compression molding technique, which consisted in compressing polymer extruded filaments into a mold leading to filament-based structures with a random porosity. The authors observed that the different internal architecture of the scaffolds did not significantly affect their degradation time; moreover, ceramic addition turned out to improve cell interaction with the material and reduce the proinflammatory effect of the degradation process.[81,82]

The osteogenic effect of β-TCP has been thoroughly evaluated by different research groups. In this regard, both Rai et al.[27] and Khojasteh et al.[83] used the same commercial PCL-β-TCP (80:20 ratio) used by Thuaksuban et al.[81] to test its efficacy on inducing mesenchymal stem cell differentiation toward an osteogenic path. The formation of mineralized matrix and the upregulation of osteogenic markers (e.g., alkaline phosphatase) were evidenced in both cases and a good integration and differentiation ability was demonstrated in vivo in rat femur[27] and dog mandible[83] models.

Hydroxyapatite (HA) is another common ceramic additive used with PCL; it is similar to β-TCP, but it presents a more developed crystalline structure, which resembles more correctly the natural structure present in the bone. HA high degree of crystallinity leads to higher elastic moduli and stiffer, more stable structures when compared to PCL-β-TCP scaffolds.[79,84] Xu et al.[85] proved the feasibility of producing an entire artificial femur to be implanted in goats, by printing PCL or PCL-HA structures with different infill and pore size to differentiate cancellous and cortical-like bone tissues (Figure 3B). The achieved porosity, less than 30%, led to mechanical properties more similar to those of the natural bone. However, the addition of a hardening phase like HA can induce relevant changes in the FDM printing parameters:[86] for example, in this case the reported printing temperature was 100 °C,[85] while typical temperatures for PCL are around 80–85 °C.[59,64] For this reason, HA can also be added after the scaffold production; for example, Lee et al.[87] coated a PCL-β-TCP FDM printed scaffold with β-cyclodextrin grafted HA and the pro-osteogenic drug Simvastatin. This structure promoted osteogenic differentiation of hADSCs in vitro and bone defect regeneration upon 6 weeks of implantation in a rabbit model.

Bioactive glass (BG) is another widely known osteoinductive and osteoconductive agent that has been used in combination with thermoplastic polymers for bone regeneration.[88] Poh et al. published two different works[89,90] in which PCL-BG composite scaffolds were successfully produced and characterized. However, in their first work the selected concentration of 45S5 Bioglass, a common commercial BG, or strontium-substituted BG (SrBG) (i.e., 10% w/w) was too low to achieve relevant osteoinductivity in the final constructs.[89] For this reason, in the subsequent study the concentration was raised to 50% w/w and the in vitro bioactivity of the scaffold improved significantly compared the PCL scaffold used as control.[90] However, the mechanical properties and especially the compressive modulus were affected by the increase in BG concentration (from 42.2 ± 3.6 MPa for PCL alone to 35.6 ± 2.5 MPa for PCL with SrBG), while this phenomenon was not observed when the scaffold was coated with calcium phosphate (41.9 ± 3.3 MPa). This issue could be ascribed to a not homogeneous dispersion of the BG particles within the PCL matrix during the composite formation, resulting in a weak interfacial bonding strength. Conversely, Wang et al.[91] recently evidenced an opposite behavior when adding different percentages (i.e., from 5% to 20% w/w) of another BG (58S) to PCL: in this case, the compressive modulus increased with the BG content (from 34.56 ± 2.14 MPa for 5% w/w to 43.52 ± 2.01 MPa for 20% w/w). A possible explanation could be the different method used in the mixing process of the two components. In the first study, the composite was obtained by adding the BG particles to a PCL solution in chloroform,[89,90] while in the second the BG component was added to melt PCL at 100 °C and stirred for 20 min,[91] probably resulting in a better dispersion of the particles. In both cases, anyway, BG particles were visible on the surface of the scaffold and good bioactivity and osteoinductivity could be observed.

Decellularized bone matrix (DBM) is another possible additive for bone tissue regeneration. It can be derived from natural bone and it comprises an organic phase, mainly collagen or other ECM proteins, together with the inorganic components. A commercial product called Bio-Oss is available, derived from

bovine source and formed by microparticles of mostly inorganic nature.[79] Hung et al.[92] produced a DBM with a formulation similar to Bio-Oss and added it to PCL, obtaining good printability at 80 °C up to a 70:30 DBM:PCL weight ratio, and promising cell compatibility and bone ingrowth in non-healing (4 mm diameter) murine calvarial defects. However, the use of an animal source to obtain the DBM could represent an issue in terms of potential pathogen transmission and body rejection. Recently, a different approach was attempted by Silva et al.,[93] that used a PCL scaffold as a support structure for in vitro culturing mesenchymal cells and inducing the natural deposition of ECM produced directly in loco. The applied cues were able to induce calcium deposition and osteogenic differentiation of the seeded stem cells after 21 days. Another advantage offered by this method relies in the possibility to derive stem cells directly from the patient.[93]

2.3. Dentistry and Oral Medicine Applications

The dental field is another popular area for FDM applications using PCL. In principle, the requirements of tooth reconstruction are similar to general bone regeneration, with the need of porous scaffolds able to promote mineralization.[94,95] Following their previous studies on bone regeneration, Park et al.[96] produced teeth replacements using PCL composites with a high β-TCP content (50% and 70%). The structures presented micropores with a size around 300 μm, with roughness and porosity dependent over the β-TCP content. This resulted in a higher capacity to absorb water (40% water uptake for 70% β-TCP content compared to 20% for pure PCL), mechanical properties similar to the natural tooth, good mineral deposition, and osteogenic differentiation capability.

However, the tooth is a complex organ composed of different tissues that also have a support function. In particular, the periodontium tissue surrounding the tooth must be considered in the replacement. This involves the regeneration of periodontal ligament (PL) fibers, the formation of cementum on the root, ligament attachment, and the regeneration of the alveolar bone surrounding the entire structure.[97–99] The first reported attempt of periodontium regeneration dates back to 2010, when Kim et al.[100] developed both murine and human anatomically shaped tooth substitutes using PCL:HA (80:20) composites, presenting 200 μm wide channels in their structure. Subsequently, a collagen hydrogel containing the stromal-derived factor-1 (SDF-1) and the bone morphogenetic protein-7 (BMP-7) filled the channels. Upon in vivo implantation, the growth factors were able to attract cells from the surrounding tissues, leading to new periodontium ligament and alveolar bone formation. Moreover, the chemotactic effect of SDF-1 on MSCs and endothelial cells was responsible for angiogenesis in the newly formed periodontium. A similar approach was followed by Costa et al.,[97] who aimed to produce a scaffold with an enhanced capability to guide the development of the different tissues forming the periodontium. The same group had previously developed a biphasic structure[101] formed by an Osteopore PCL:β-TCP (80:20) scaffold and a solution electrospun membrane based on the same polymer to replace the bone section and the periodontium, respectively. PL cells and osteoblasts were also incorporated within the construct in the form of cell sheets. However, although the scaffold enhanced cell sheets stability, the bone compartment did not result in a satisfactory bone regeneration. Thus, in the subsequent study, the authors applied a coating containing calcium phosphate to the structure and produced the membrane by melt electrospinning, resulting in larger pores, increased porosity and better integration between the two scaffold sections. After these improvements, better bone ingrowth and mineralization were observed, along with new vascularization and more physiological fiber orientation.[97] Finally, Lee et al.[98] designed a three-phase scaffold with different microstructures generated by printing a PCL:HA (90:10) composite forming 100, 600, and 300 μm wide microchannels, to mimic cementum, PL, and alveolar bone, respectively. The three phases also incorporated PLGA microparticles, encapsulating the best suited biological cues for each compartment (i.e., amelogenin, connective tissue growth factor (CTGF) and BMP-2) and dental pulp stem cells (DPSCs) suspended in a collagen matrix. The murine in vivo study showed that the different signals provided were able to guide stem cells toward the correct differentiation paths in the three compartments of the scaffolds.[98]

2.4. Cartilage Tissue Engineering Applications

Although the majority of PCL applications are directed toward hard tissues such as bone or teeth, there are also studies that focus on soft tissues,[102] especially cartilage. PCL is particularly attractive for those applications that require a good load bearing capacity, such as knee joints and meniscus substitution and regeneration. Szojka et al.[103] produced 3D printed menisci with pure PCL, exploiting the ability of FDM to reproduce complex geometries. Their aim was to obtain a patient specific structure and a good recapitulation of the collagen I fibers orientation in the native tissue, mimicked by printing the polymer filaments combining grid and circular designs. Although the mechanical properties of the fabricated scaffolds were finely tuned acting on layer architecture, the obtained compressive modulus values were decidedly different from the physiological ones (tens of MPa against tens of kPa).[103] Interestingly, the authors also included a suture strategy to secure the implant to the tibial plateau to improve stability and accelerate the healing process. As for bone tissue engineering, most studies focus on coupling the use of PCL with additives or scaffold fillers. For example, Zheng et al.[104] conducted an in vivo study in rabbits using a scaffold obtained by a composite of PCL:nano hydroxyapatite (70:30 weight ratio). Moreover, they coated the scaffold with a co-suspension of umbilical cord blood derived MSCs (UCB-MSCs) and chondrocytes immediately before implantation. The authors were able to qualitatively demonstrate that the growth factors secreted by these cells promoted both cartilage and subchondral bone regeneration.

However, the most common strategy to promote cartilage regeneration combines a thermoplastic-based structure, able to provide support and adequate mechanical properties, with a hydrogel filler, which can generally offer a more cell-friendly environment for cell proliferation despite being too weak to be used alone.[105] Similarly to Zheng et al.,[104] another group aimed to obtain the simultaneous regeneration of the cartilage tissue and the subchondral bone. They developed a copolymer of PCL and methoxy poly(ethylene glycol) (mPEG) (acronym of the copolymer mPEG-PCL) used in combination with hydroxyapatite to

reproduce the bone compartment. Then, a hydrogel based on methacrylated hyaluronic acid was loaded with the transforming growth factor β_1 (TGF-β_1) and deposited on the outer layer of the scaffold using photoreticulation, to mimic the cartilage environment. An in vivo study in swine demonstrated a successful healing of a cartilage defect in the animal's knee, also resulting in a more hyaline-like cartilage appearance compared to controls (no scaffold implantation).[106]

Van Uden et al.[107] developed an intervertebral disk (IVD) substitute composed by an FDM PCL scaffold, with a design obtained from anatomical imaging of the patient, and a methacrylated gellan gum hydrogel hosting autologous nucleus pulposus cells. Rabbits' IVDs scans were obtained by microcomputed tomography (μCT) and successfully replicated through FDM, reaching compressive stiffness three to four times higher than the native tissue, both in dry and wet conditions (5.9–6.7 and 1.73 kN mm^{-1}, respectively). Wang et al.[105] combined a PCL scaffold with a PLGA–PEG–PLGA thermogel, able to undergo a phase transition from sol to gel at 37 °C and used to encapsulate bone marrow MSCs. Remarkably, this group noted an initial faster cell attachment and growth on the native PCL scaffold in the absence of the gel. However, the use of the thermogel turned out to permit better cell retention and proliferation, avoiding cell aggregation on the outer surface of the scaffold. Moreover, the combination of the two components led to an elastic modulus (45.3 ± 16.5 MPa) comparable to the natural osteochondral tissue (45.1 ± 10.3 MPa) and induced MSC chondrogenic differentiation in vitro.[105] In another study, Visscher et al.[108] created an ear substitute in which an outer layer of printed PCL was used to provide mechanical stability and a 3D framework to host hydrogels seeded with cells. They demonstrated that the PCL cage prevented the shrinking of a fibrin/hyaluronic acid-based hydrogel containing both adipose stem cells and perichondrocytes. Furthermore, cells deposited an ECM suitable for new cartilage formation at a rate compatible with the cage degradation, also sustained by an increase in the Young's modulus over time due to the new matrix deposition.[108]

2.5. Other Biomedical Applications

Bone and cartilage reconstruction are undoubtedly the most explored fields for PCL scaffolds; however, many studies are also present regarding different tissue engineering applications, due to the versatility on mechanical properties and degradation rate achieved using 3D printing techniques. An interesting example in this sense is given by trachea reconstruction.[109] As trachea is a complex organ which functioning is essential for living, its reconstruction and regeneration are a delicate topic to address. Although trachea main component is cartilage, connective tissue is also present to guarantee bending and expanding of the pipe during breathing and neck movements. Another important aspect is the colonization by the ciliated respiratory epithelium, that ensures the mucociliary clearance.[24] Moreover, the trachea is not cylindrical, but rather a multilayered structure composed of 15–20 C-shaped cartilage disks. For this reason, 3D printing techniques are particularly suitable for its reconstruction and many studies have thus concentrated on this topic.[110–112] Chang et al.[24] produced a C-shaped scaffold with 300 μm regular pores using PCL, then coated with fibrin-immersed MSCs. The scaffold was implanted in rabbits to fill a tracheal defect and the scaffold mechanical properties turned out to be adequate for the application since no stenosis of the canal occurred; furthermore, a good presence of ciliated epithelium was observed together with new cartilage formation. Park et al.,[113] on the other hand, concentrated on the printing technique to achieve a better shape fidelity to the native trachea: they combined a traditional 3 axis printer with an additional rotational structure, around which the tubular structure was printed. Comparing this structure with traditionally printed ones, they reached better fidelity to the CAD design, more uniform pore size and PCL fibers shape. Invivo experiments in rabbits also confirmed the suitable mechanical properties and biocompatibility of the fabricated scaffold. Other in vivo studies regarding the use of PCL in tracheal surgery are reviewed elsewhere.[109] PCL was also used as a building block for a thermoplastic poly(ester urethane), intended for trachea reconstruction in combination with a poly(ether urethane).[114]

As for to the trachea, also vascular grafts need to be produced in circular shape. Similar to Park et al.,[113] Centola et al.[115] employed a cylindrical plate used as a rotating mandrel to produce 5 mm wide hybrid scaffolds, formed by an electrospun heparin-encapsulating poly(L-lactic acid) (PLLA) membrane and a PCL coil obtained by FDM as an outer strengthening layer. Results demonstrated that the PCL armor enhanced the mechanical properties of the electrospun scaffold in terms of elasticity and compliance, also permitting an in vitro heparin release and differentiation of MSCs seeded on the graft.[115]

As previously noted, PCL lower T_m compared to other thermoplastic polymers makes it suitable for incorporating biologically active substances that can tolerate moderately high temperatures. For this reason, some drug delivery devices have been developed using FDM printers, although some issues are still under consideration. Earlier experiments such as the one performed by Rai et al.[116] did not incorporate the drug directly within the scaffold, but added the biomolecule, in this case recombinant human BMP-2 (rhBMP-2), after production, aided by a fibrin adhesive. Although this type of drug incorporation ensured the retention of protein bioactivity, the maximum loading efficiency obtained was 73% and the release profile was characterized by a relevant burst release (up to 53.3% in the first 24 h), caused by the dissolution of fibrin in physiological conditions.[116] By directly incorporating the drug within the PCL structure, on the other hand, it is possible to obtain greater drug loading efficiency, between 73% and 90% as reported by Holländer et al.,[117] with a certain loss due to drug retention on the surface of the melting pot during filament fabrication. In this case, the aim was to produce an intra-uterine system able to release a contraceptive drug, indomethacin. The release was sustained for 30 days with an appropriate rate for the considered application, although the presence of the drug influenced the filament morphology, since indomethacin tended to crystallize during storage. A comprehensive study on drug loading within different thermoplastic polymers was performed by Kempin et al.[30] In general, the release kinetics is strongly dependent on the polymer used, but also on the quantity of drug loaded into the device. As demonstrated using FDM printed PCL, the released percentage of quinine was progressively higher when the loaded drug raised from 2.5% to 25% w/w. In addition, the authors also reported a considerably longer drug release when compared to the previously mentioned studies (up to 56 days).[116,117]

Meshes are a popular architecture in regenerative medicine, because of their versatility and ease of production since they are comprised of a limited number of layers. For instance, Teo et al.[118] developed PCL:β-TCP (80:20) honeycomb structures containing different percentages of antibiotic agents for wound healing applications. The release reached a maximum value of 93% after one week for the highest drug loading (25% w/w) and efficacy against both Gram-positive and Gram-negative bacteria was observed in vivo up to 7 days. For surgical meshes, Ballard et al.[119] addressed the problem of imaging visualization of structures after implantation by printing PCL grids containing CT contrasting agents. Good retention of drugs was obtained, and barium-loaded scaffolds were able to retain visibility in a physiological milieu for several days.

3. Poly(lactic acid)

Poly(lactic acid) (PLA), also known as polylactide, is one of the most common aliphatic polymers not only in 3D printing, but for biomedical applications in general. It is a thermoplastic polymer, with generally high elastic modulus values in the order of a few GPa.[120,121] Furthermore, it is an environmental friendly material as it can be obtained from renewable sources, such as sugars and organic acids.[122,123]

Due to the chiral nature of the constituent lactic acid, PLA presents three stereoisomers: PLLA, poly(D-lactic acid) (PDLA), and poly(DL-lactic acid) (PDLLA). The distribution of these enantiomers along the polymer chains strongly influences its mechanical properties. In particular, pure PLLA or PDLA have a higher degree of crystallinity, while mixed isomers composition leads to amorphous structures.[21,124] Amorphous PLA (i.e., PDLLA) is easier to process by casting, molding, or extrusion, but the absence of crystalline domains detrimentally affects its strength. For crystalline PLAs (i.e., PDLA and PLLA), T_m reaches values between 190 and 250 °C, while T_m can decrease to 130 °C and T_g to 60 °C when crystallinity decreases. Molecular weight and thermal history can also affect these parameters.[21,125–127]

PLA is generally a hydrophobic and brittle material, with 10% maximum elongation at break; it also presents a long degradation time in vivo, that can reach several years (from 2 to 8) depending on its characteristics.[128,129] Additionally, PLA is generally recognized as safe[125] and used for a wide range of biomedical applications, from sutures to tissue engineering scaffolds and disposable surgical instruments.[130–133] Medical grade PLA is readily available on the market,[134] also in ready-to-print filaments.[135]

3.1. Scaffold Parameter Optimization

PLA has been extensively studied for FDM applications. Hence, many groups have investigated its properties and suitability to obtain scaffolds of different architectures and complexity.[6,122,136] One of the first aspect to consider in the manufacturing of PLA is the influence of the processing method on the material biocompatibility. Wurm et al.[137] cultured osteoblasts on printed PLA disks and reported the absence of any cytotoxic effect (95.3% ± 2.1% of cell viability). They obtained even better results than with cells cultured on titanium surfaces, which compatibility toward osteoblasts is well known. A similar good result with PLA-based FDM constructs was also reported in another study,[133] which demonstrated that PLA presents better proliferation rate when compared to other commonly used polymers, such as PCL or poly(dioxanone). Additionally, a higher biocompatibility was observed when the polymeric chains were composed only of L-lactic acid units instead of both enantiomeric forms.

A study by Cicala et al.[138] compared different commercially available PLA filaments to understand how their properties affected the quality of the final printed structures. Interestingly, the main result was that pure PLA filaments are not suitable for FDM applications, especially with regard to the possibility to print complex geometries and overhanging structures, i.e., suspended parts obtained without the use of a supporting material. High viscosity and presence of fillers seem to be the most important factors to obtain appropriate rheological behavior and tensile properties in the final printed objects.[138] In accordance with these results, Wang et al.[139] demonstrated that PLA reinforced by Bamboo powder, calcium carbonate, and cellulose, both in the form of crystals and fibers (20% w/w for all the compositions), showed better mechanical properties than pure PLA. By adding $CaCO_3$, Young's modulus increased up to almost 60%. Better results could also be achieved by mixing fillers and PLA directly in the printing system rather than first creating the composite and then processing the resulting material.[139] Other fillers that could be embedded successfully in PLA are metal–organic frameworks (MOFs), which open up toward different applications, from catalytic to sensing applications. Evans et al.[140] incorporated up to 40% w/w of MOFs inside PLA structures, resulting in improved mechanical properties and a complete preservation of the MOFs chemical sensitivity, thanks to their crystalline nature that allowed them to be processed at the normal PLA printing temperatures (i.e., within the range 180-230 °C).

Another important issue to address regarding the printing of PLA is its general stiffness, which can result in poor flow properties and therefore difficulties in the printing process. While high viscosity can be useful in providing good mechanical properties to the final constructs, it can result in nozzle clogging and defects on the scaffold surface. A possible strategy to overcome this issue lies in the use of plasticizers, which can significantly improve PLA thermal and mechanical properties. Carlier et al.[22] studied the effects of four different plasticizers (PEG 400, triacetin, triethyl citrate, and acetyl triethyl citrate, 10% w/w) on different processing parameters. Both T_m and T_g were significantly lowered by the plasticizer addition, so that the printing temperature could be reduced from 180 °C for pure PLA to a minimum of 135 °C when PEG 400 was used, while maintaining a good thermal stability. Plasticizers also increased the blend plasticity, resulting in lower Young's modulus and tensile strength values, which are generally beneficial for implant integration within body tissues. A copolymerization between PLA and PCL was also attempted.[61] The resulting material, however, turned out to be more difficult to print than pure PCL and PLA (Figure 3A), requiring the application of a higher pressure and an extruding temperature of 190 °C.[61]

For FDM processes, surface finishing is one of the most important limitations. As reported by several authors,[128,138,141,142] the deposition of subsequent layers often results in uneven outer surfaces because the printing resolution cannot be exactly

matched by the filament. Roughness influences not only the aesthetic of the surface, but also mechanical properties can be impacted, especially tensile strength.[8] It is possible to obtain better surface finishing by pre-processing intervention, i.e., by changing the printing parameters or adjusting the polymer properties. However, sometimes only post-processing treatments can be performed, either by mechanical or chemical means. Valerga et al.[143] attempted a chemical treatment by immersing printed scaffolds in organic solvents (ethyl acetate, tetrahydrofuran, dichloromethane, and chloroform) for 30 or 60 s. Roughness reached values around 97% using chloroform and a further crystallization formed on the surface, resulting in a strengthening of the entire structure. Nevertheless, there was a partial retention of the solvent, which is undesirable in view of using scaffolds in biological environments.[143] Topography is also an important cue to consider when cells are involved, since it is known to play a role in guiding proliferation and differentiation. Feng et al.[144] explored roughness on FDM manufacts not only at the macroscale but also at the nanoscale, studying its effect on dental pulp derived cell differentiation. They compared 3D printed and molded disks, which main difference resided in surface smoothness. Indeed, the printed samples presented an uneven surface with a multi-scale roughness resulting from the quick cooling of the filament upon extrusion from the nozzle, whereas the molded disks exhibited a smooth surface. Dental pulp cells proliferation was not affected by the surface morphology, but an effect on differentiation was evident: cells on molded, smoother surfaces exhibited osteogenic markers after 42 days of culture, while printed matrices supported an odontogenic path.[144] Hence, surface morphological modification must be taken into account to provide the right cues to the cells interacting with medical devices.

3.2. Bone Tissue Engineering Applications

Similarly to PCL, also PLA preferred applications are related to bone substitution and regeneration, given its mechanical properties and slow degradation rate.[145] Moreover, although PLA itself does not possess any osteogenic potential, its bone compatibility is well known.[133,146,147] For example, Gremare et al.[148] produced 200 μm thick porous scaffolds for bone tissue engineering, showing different pore sizes (150–250 μm) and a good CAD fidelity and reproducibility. Furthermore, they demonstrated that despite the processing significantly modified PLA properties in terms of molecular weight (average molecular weight loss about 48%) and degradation temperatures (lowered from 293 and 370 to 250 and 363 °C, respectively), the final scaffold was still compatible toward human bone marrow stem cells.

To provide PLA-based scaffolds with better osteogenic properties, the well-known strategies of mineral addition and surface modification are usually employed. As already shown for PCL, hydroxyapatite is used both to strengthen the polymeric structure, in particular regarding recovery stress and strain, and to improve biocompatibility and osteoconductivity. Another remarkable effect of HA is the ability to act as a buffer for the acidic byproduct of PLA degradation, that could be dangerous for the cell environment.[149] Chen et al.[150] reinforced PLA filaments for FDM adding 10% w/w of nanometric HA. The structure presented pores around 300 μm and ultimate stress similar to the natural trabecular bone (23 MPa vs. 1–12 MPa), in vitro and in vivo biocompatibility and ability to successfully integrate into bone defects after 12 weeks. Despite this good results, hydrophobicity remained a relevant issue, resulting in a failed attempt to adsorb an antibiotic on the scaffold surface.[150] Another group addressed this problem by coating a PLA scaffold using poly dopamine.[146] This strategy permitted to improve the surface hydrophilicity and successfully attach BMP-2, which resulted in higher cell adhesion, osteogenic differentiation and mineral matrix deposition. A better performance of printed scaffolds with respect to traditionally manufactured ones was also observed, regarding in particular pore interconnection and release of lactic acid byproducts during degradation. Studies on the use of bioactive glass in combination with PLA are also present in the literature. Estrada et al. demonstrated the in vitro bioactivity of scaffolds printed using a filament produced by mechanically grinding and mixing PLA and 45S5 BG.[151] More recently, standard filaments of this same composite with BG percentages ranging between 1% and 10% w/w were developed by Distler et al.[152] and used to obtain scaffolds able to induce osteogenic differentiation in vitro. However, as also noted by other authors,[89,90,153] an improper interface adhesion between the polymer and the BG was present, resulting in a decrease in the compressive strength of the scaffold starting from 2.5% w/w BG concentration. Moreover, the resolution of the printing process was also affected, originating from variability in the starting filament diameter: further improvements in the interface binding between the fillers and the polymer are thus needed. Better results in this sense were obtained by several groups using plasticizers such as PEG[153] or solvents,[154,155] but this process can sometimes hinder the final structure biocompatibility.

Since PLA has been widely studied as a material for FDM applications, the latest research trend has been focused on producing more anatomically accurate scaffolds rather than traditional, proof-of-concept architectures with evenly distributed pores. Buj-Corral et al.[46] developed a computational model to design structures with different levels of material density within the scaffold and a random porosity. The porous planes design included geometries optimized for bone tissue applications, joined by a number of columns. The FDM prototypes produced using PLA showed satisfying reproducibility, but mechanical properties were not investigated fully. Additionally, too thin columns could not be printed in standard conditions, so that the prototypes had to be scaled of a factor five with respect to the desired dimensions, suggesting the need for further optimization.[46] Pecci et al.,[28] on the other hand, designed a bone ECM-like structure by finely controlling geometry via FDM and mechanically characterized the produced structs. They studied different pore sizes, resulting in different porosities (maximum value 65% for 600 μm pores) and mechanical strength values, that resulted to be comparable to other results found in the literature.[28] Additionally, Wu et al.[156] produced a PLA/HA scaffold reproducing the trabecular femoral bone architecture, with HA content ranging from 5% to 15% w/w (**Figure 4**A). A difficulty in reproducing the trabecular morphology was found with increasing HA content, with negative effects on the mechanical properties of the finally structs, that moved toward the lower range of the values reported for trabecular bone.

In all these studies, no biological assessment was conducted; hence, no data on the biocompatibility of these complex

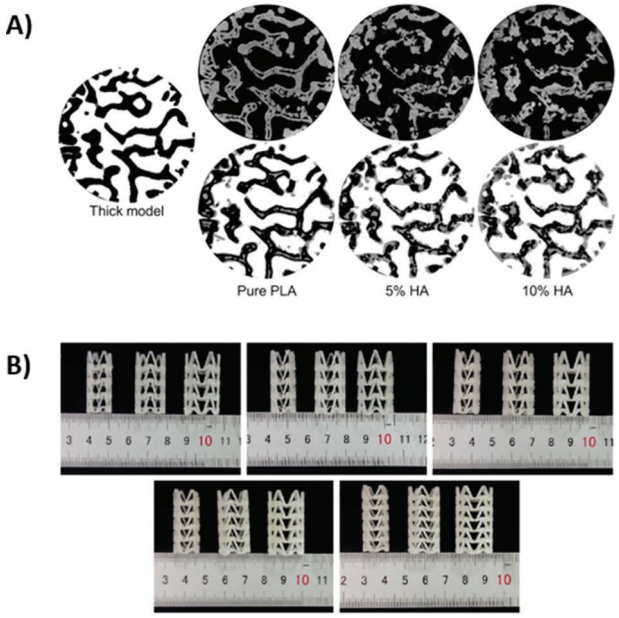

Figure 4. Application of FDM-processed PLA in different medical fields. A) Scaffolds for bone tissue engineering containing different HA percentages (pure PLA = 0% HA) reproducing the trabecular architecture of the femur. Adapted with permission.[156] Copyright 2020, Elsevier. B) PLA vascular bioresorbable stents with shape memory properties. Reproduced under terms of the CC-BY license.[157] Copyright 2018, The Authors, published by MDPI.

structures are available. Additive integration and mechanical properties modulation also need further optimization. Finally, another possible strategy to improve the biomimicry of the native bone tissue was pursued by Sears et al.[158] They designed a multimaterial setup to print simultaneously a fumarate-based ink, with excellent porosity and permeability, and a PLA external layer, to provide the required mechanical strength for bone grafts. This approach resulted in an enhanced biocompatibility while maintaining compressive values and yield strength in the range of trabecular bones.[158]

3.3. Drug Delivery Systems

FDM is not traditionally employed in the pharmaceutical field; however, a certain interest has raised in this sense over the last few years. The main advantage of using this technology in this field lies in its high versatility, that for example permits to obtain personalized tablets with dimensions and dosages tailored to the single patient needs.[159] Even more interesting is the possibility to print implantable drug delivery devices that can be produced according to the patient's anatomy, with complex geometries difficult to obtain otherwise.[160,161] Regardless of the device shape, there are two methods to incorporate drugs into FDM printed structures. The first involves a direct mixing of the drug with the polymer powder before extruding the filament, while the second comprises the soaking of the printed devices in an appropriate drug solution enabling polymer swelling without dissolving it. This latter method allows to better preserve drug activity, since it avoids the high temperatures usually needed for the printing process. However, the drug loading obtained by mixing the agent before printing is significantly greater.[30] The first examples of drug delivery systems produced by FDM were made of poly(vinyl alcohol),[162–166] and other devices have been produced using PCL, as mentioned before.[116,117]

Regarding the use of PLA, drug-loaded 3D printed catheters were produced mixing PLA, gentamicin sulfate, and dexamethasone in pellet form before printing, to obtain both an antibacterial and chemotherapeutic effect.[167] Catheters showed a sustained payload release over 5 days in simulated biological environment and relevant antibacterial activity in culture broth. Luzuriaga et al.,[168] on the other hand, printed an array of microneedles to deliver drugs transdermally and exploited the second method to load therapeutic agents. The needles were pyramid-shaped, with a width between 400 and 600 μm and a height between 200 and 2500 μm. The payload was loaded by soaking the needles into acetone solutions containing methylene blue and fluorescein as model drugs easy to visualize and quantify. A sustained release was observed up to 12 h.[168] Finally, the two strategies were combined in a further study to produce a double drug delivery scaffold.[169] This group added dexamethasone during the PLA filament production and prednisolone after the manufacturing process, by soaking the structures into a 50:50 methanol:ethyl acetate solution containing the drug (**Figure 5**). The combination of the two strategies permitted to obtain two different release profiles: prednisolone was completely delivered in one week, with a burst release (80% of the payload) in the first day, while dexamethasone slowly released in four months. In this study, also cytocompatibility and anti-inflammatory activity were evaluated.[169]

3.4. Other Biomedical Applications

Other applications of PLA processed using FDM can be found in dentistry. Beside teeth substitutes, able to regenerate the surrounding environment as shown for PCL,[96–98,100] complete denture production is also a possibility. Metal powders or resins manufactured by milling are the traditional choice in this case. Anyway, the fidelity to patients' anatomy reached using CAD guided printing and the ease in the production methods are particularly attractive in the dental field. Deng et al.[170] developed a complete denture printed using PLA, obtaining a fidelity comparable to traditional resin prostheses and a better adaptability during the positioning phase (PLA could be softened by immersion in water at 100 °C) and artificial teeth insertion. Moreover, costs can be significantly reduced, along with the time needed to produce the complete denture, i.e., 1 h for the sample hollow structures used in the study.

Vascular stent production commonly uses PLA, which is a resorbable material, avoids restenosis and is more suited to narrow vessels compared to metals.[171,172] Some attempts to obtain polymeric stents have also been made using rapid prototyping techniques, often embedding active agents into the structure to produce drug eluting stents.[173–175] Wu et al.[157] produced an FDM-printed PLA stent with an arrow-shaped structural unit, studying how its geometry and characteristics influenced mechanical and shape memory properties (Figure 4B). Devices with a 12 mm diameter and 1.8 mm thickness showed the best compressive modulus and radial force resistance for application as vascular stents.

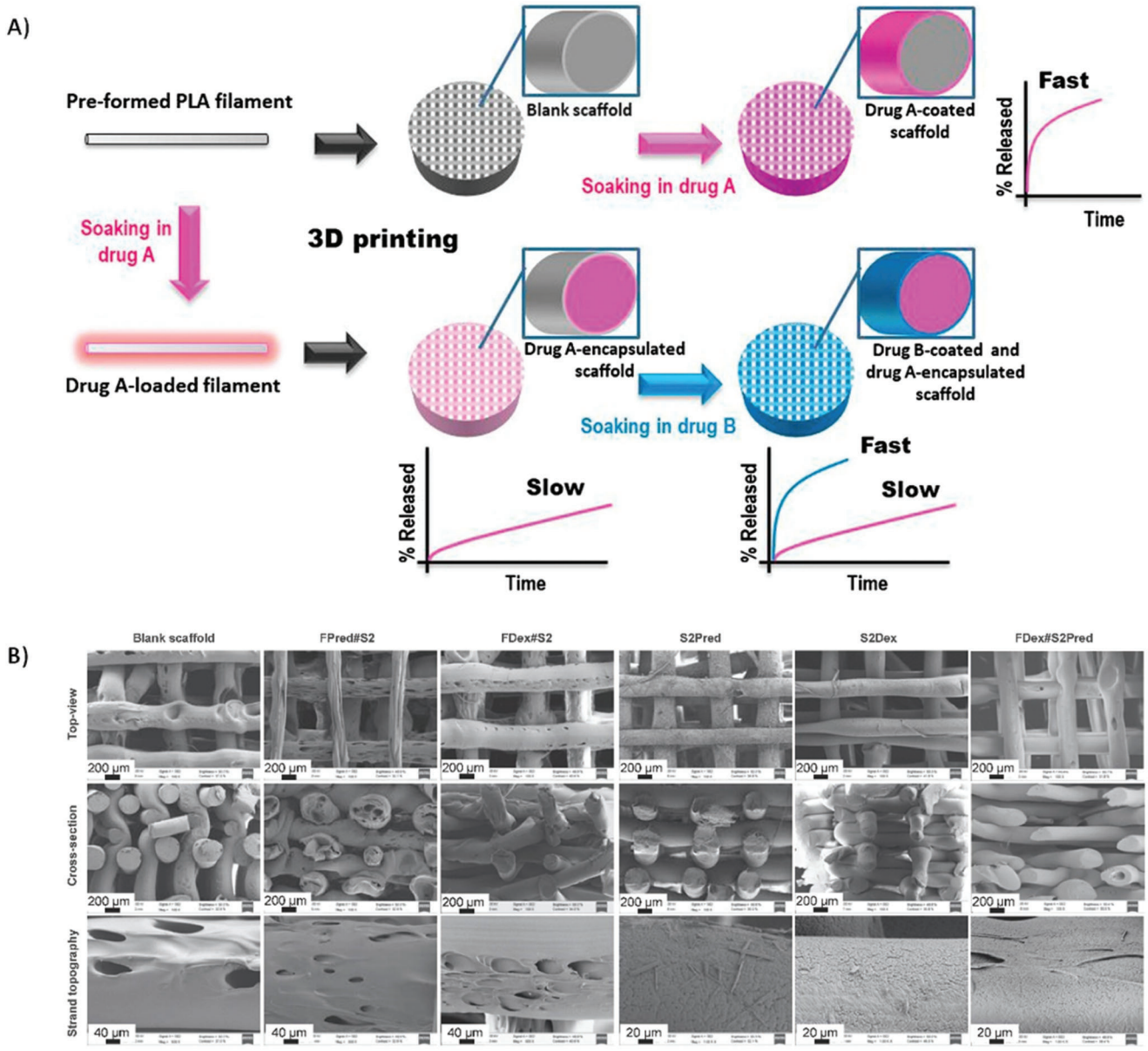

Figure 5. Drug delivery performed with FDM-printed PLA structures. A) Schematic representation of different methods of drug encapsulation: (i) soaking of printed-structures in a drug-solution (top image), and (ii) double loading approach, combining drug A encapsulation during the filament processing and the soaking of the resulting structures in a solution of drug B (bottom image). B) SEM images of the printed structures, with different drugs and methods of encapsulation (FPred#S2: prednisolone-loaded filaments; FDex#S2: dexamethasone-loaded filaments; S2Pred: structures soaked in prednisolone solution; S2Dex: scaffolds soaked in dexamethasone solution; FDex#S2Pred: dual loaded structures). Reproduced with permission.[169] Copyright 2019, Elsevier.

The ability to simultaneously increase the diameter and shrink longitudinally was confirmed, along with a shape memory effect at temperatures lower than PLA T_g (i.e., also at 37 °C, that is the temperature of interest for stent implantation).[157]

Poly(lactic acid) and poly(glycolic acid) have been extensively used in the surgical field to produce resorbable sutures and grafts. An interesting application in this sense could be the printing of surgical instruments, both disposable and reusable, to minimize the cost and allow for a fast, customized availability. Rankin et al.[132] attempted to print an Army/Navy retractor for human tissues using PLA. The printing process was fast and cost-effective ($0.46 for each retractor), and the resulting objects were able to sustain a load adequate for surgical interventions (13.6 kg) and suitable for sterilization with glutaraldehyde with no impact on material strength and properties even after repeated cycles.

3D printing is an interesting manufacturing technique also in sensor system production, in particular in the field of electrochemical analysis. This interest raises mostly from the possibility to create customizable electrodes, thus facilitating handling and assembly of the final devices.[176,177] Carbon-based filaments

for FDM can be easily produced by mixing polymers and carbon sources in powder form. Plastic-based electrodes are nowadays preferred to metal-based ones because of their reduced cost and better production setups.[178,179] A commercial graphene/PLA filament was used by Manzanares-Palenzuela et al.[180] to produce electrodes in the shape of rings or disks, able to sense the presence of picric and ascorbic acid. The electrodes were activated by dipping them in dimethylformamide for 10 min, which resulted in a partial dissolution of the superficial PLA. After this modification, the sensitivity of the system increased, and the two acids were detectable spanning almost two orders of magnitude of concentration (i.e., in the concentration range from 10×10^{-6} to 500×10^{-6} M). Richter et al.,[181] on the other hand, designed a complete system formed by an ABS electrochemical cell with a 5 mL volume and working and reference electrodes obtained by a carbon black and a PLA filament. Also in this case, a partial etching of PLA on the surface of the electrodes using a 0.5 M NaOH solution resulted in better performances. Both organic and inorganic substances were successfully detected, with results comparable to traditional platinum and Ag/AgCl electrodes.[181] The application of these technologies in the biomedical field could be devoted to biosensing[182] or biopotential measurements.[183]

4. Other Polyesters for FDM Applications

Although PLA and PCL are by far the most studied materials for 3D printing, also other polyesters have found application in this field. Among them, the copolymer PLGA and the family of PHAs are particularly relevant for biomedical use. Moreover, also thermoplastic polyurethanes (TPU)s that comprise ester blocks within their backbone have gained interest. Indeed, several of them have already been developed as commercial filaments that can be used with common printers without further preparation.

4.1. Poly(lactic-*co*-glycolic acid)

The copolymer formed by lactic acid (LA) and glycolic acid (GA) is one of the most employed polymers in biomedical applications, thanks to its suitability to a wide range of manufacturing techniques[184] and availability in the medical grade.[185,186] Common examples are micro- and nanoparticles for drug delivery,[187,188] and electrospun mats targeting the repair and regeneration of various tissues.[189–191] The reaction between lactic acid and glycolic acid has the main purpose to regulate the hydrophilicity of the final polymer. PLA is more hydrophobic than PGA, because it presents a methyl group in its repeating unit that PGA does not contain. Moreover, by combining these two building blocks, it is possible to control hydrolysis rate and thermal properties and achieve different degrees of crystallinity. Usually, when the lactic acid content is lower than that of glycolic acid, the final polymer is more amorphous and the degradation rate increases.[192,193] PLGA melting temperature (225–230 °C) is higher than the typical values reported for PLA (173–178 °C), but its T_g is considerably lower (35–40 °C against 60–65 °C for PLA).[26]

In FDM applications, PLGA is rarely used as unique struct forming material due to its poor thermal stability. Compared to other linear polyesters, PLGA is more susceptible to thermal degradation during the printing process, resulting in a marked molecular weight reduction and high polydispersity index.[194] Loss in mechanical performances and fast degradation are typical consequences of this change in chemical properties. Shim et al.[16] systematically studied the degradation effects of exposing PLGA (LA:GA ratio 85:15) to 120 °C for relatively long periods of time (from 1 to 7 days). They observed a significant reduction of the molecular weight: starting from a $\overline{M_n}$ around 80 000 Da, after 1 day it was reduced to 30 000 Da, finally reaching a value of 8000 Da after 7 days of heat exposure. In addition, the T_g of the amorphous phase also shifted toward lower values. Although scaffolds produced in all the mentioned conditions maintained good resolution and printing fidelity, the hydrolytic degradation was considerably faster for PLGA subjected to longer heating. The thermal history also affected the viability of cells seeded on the scaffolds: after 3 days, osteoblast progenitors showed poor proliferation during culture on the faster degrading scaffolds. This could be ascribed to the acidic by-products given by PLGA degradation, which production represents a known issue with this material and is more pronounced in the presence of short chains produced by the thermal degradation.[16,195] To facilitate the removal of these acidic degradation products, Hung-Jen et al.[194] tried to create larger pores (1.15 mm) inside the scaffolds, in order to improve the washing out of waste products that could be detrimental for chondrocyte viability. Scaffolds were also filled with type II collagen to induce better cell survival and attachment, and the structures turned out to be still suitable for cartilage regeneration, despite the loss of mechanical stability given by the relevant porosity.[194]

The technical demand of providing PLGA scaffolds with high porosity values was also observed by Kim et al.[196] They noted that their HA-coated scaffolds based on PLGA/TCP nanocomposites, having a porosity <60%, did not support new bone formation even after 12 weeks of implantation in vivo. Especially for bone regeneration, a correct balance between porosity and mechanical properties is required to concurrently sustain mechanical loads and drive tissue regeneration; for these reasons, a slow-degrading polymer like PCL is generally preferred for bone tissue engineering applications.[58]

Recently, Feuerbach et al.[186] studied the possibility to obtain standard filaments (1.75 mm ± 0.05 mm) for FDM using commercial, medical-grade PLGAs with differing LA:GA ratios. As previously mentioned, molecular weight and Young's modulus are important parameters for polymer processability: brittle materials (e.g., PLGA with 75:25 LA:GA ratio, molecular weight lower than 15 kDa) were unable to give filaments with proper mechanical performances and structural stability.[16,186] Another group[197] started from the same commercial PLGA with a 50:50 LA:GA ratio to produce filaments and produce FDM printed implantable systems for the release of monoclonal antibody (mAb). In this case, to overcome the difficulties already mentioned for PLGA, they added PEG as plasticizer (6.6–7.6% w/w). The mAb was added in the form of spray-dried powders with different stabilizers to preserve the functionality also at the elevated printing temperatures (105 °C). However, even the most promising formulation (containing D-(+)-trehalose dehydrate and L-leucine as stabilizers for mAb powders) was only able to maintain an mAb functionality ≈70%, thus requiring further optimization of the encapsulation process.[197]

4.2. Poly(hydroxyalkanoate)s

PHAs are a family of polyesters gaining a raising interest in many fields, including the medical one. They are known for their biocompatibility and biodegradability with non-toxic by-products, and they exhibit characteristics similar to synthetic polymers despite their natural origin.[21] They are synthesized by bacteria in particular culture conditions (especially low oxygen and enhanced carbon sources). For this reason, they are considered environmental friendly materials compared to conventional petroleum-based plastics.[198,199] Depending on the carbon source fed to bacteria, different types of PHAs can be obtained, differing in the side chain length. The most relevant PHAs for biomedical applications are short chain length (3-5 carbon atoms in the side chain) (e.g., poly(hydroxy butyrate) (PHB) and the copolymer PHBV) and medium chain length (5–14 carbon atoms) (e.g., poly(hydroxy hexanoate) and poly(hydroxy octanoate)) PHAs. PHB and some of its copolymers can also be purchased in the medical grade.[200,201] However, many PHAs used in medical research are still produced only on a laboratory scale; hence, this aspect needs to be assessed on a case-by-case basis. PHAs with short side chains are generally brittle and stiff; however, their copolymerization, as in the case of PHBV, leads to mechanical properties more suitable for industrial processing.[202] Still, one of the most impairing issues regarding PHAs is their thermal instability; for example, PHB has a T_m around 180 °C and degradation phenomena start at 220 °C, resulting in a narrow temperature window for processability. Thus, plasticizers as well as different types of fillers and additives are generally added to avoid decomposition and improve melt resistance.[203] This strategy is also useful to diminish costs, which are one of the most relevant obstacle for PHA diffusion in the industrial production.[204]

Regarding FDM applications, the literature reports only few examples on the melt processing of PHAs, mostly due to the problematics previously identified. Nevertheless, a research group developed several types of standard FDM filaments (1.75 mm ± 0.05 mm) using a commercial PHA (EM 5400F, Shenzen Ecomann Biotecnology Inc.), with different additives.[204–206] In all cases, a better compatibility between the additive and the polymeric matrix was achieved by grafting the PHA with maleic anhydride (PHA-*g*-MA). In the first work, modified multiwalled carbon nanotubes were incorporated in the matrix to produce the filaments.[205] Improved mechanical and thermal properties (initial decomposition temperature improved by more than 70 °C) were obtained with a 1% w/w filler content, along with antistatic (electrical resistivity 10^8 times lower than the polymeric matrix alone) and antibacterial properties. Afterward, the same group focused on fillers derived from natural sources and wastes, in an effort to be more environmentally conscious and lower production costs. Wood flour (WF), with antimicrobial, deodorizing and anticancer properties,[204] and palm fibers (PFs), a byproduct of palm oil production,[206] were used to achieve these goals. Both additives showed the best results at a 20% w/w concentration. This is a relatively high amount for an additive, which resulted from the good adhesion between the particles and the polymeric matrix thanks to the MA grafting. Compared to pure PHA, composites showed better tensile strength and Young's modulus. The presence of WF was also able to lower the T_m of about 5 °C and improve water resistance and antibacterial properties.[204] On the other hand, PFs improved water absorption and biological degradability (25% weight loss for PHA *vs.* 40% for PHA-*g*-MA/PFs after 60 days), and showed no cytotoxic effects on fibroblasts.[206] A similar study was conducted by Valentini et al.[207] that designed a novel composite using poly(3-hydroxy butyrate-*co*-3-hydroxy hexanoate) and fibrillated nanocellulose. In this case, they were able to incorporate only 0.5% w/w of additive without impairing adhesion with the polymeric matrix and forming aggregates. However, even this small quantity of cellulose improved elongation and tensile strength of the produced filaments of about 10%.[207]

In all the previously mentioned studies, filaments for FDM were successfully produced and characterized, but no proof-of-concept of their printing potential was reported. Conversely, Ye et al.[208] printed PHBV-based scaffolds via FDM and characterized them for bone tissue engineering applications. First, they produced PHBV/calcium sulfate hemihydrate (PHBV/CaSH) composites and obtained filaments by a twin-screw extruder. Then, scaffolds with a 400 μm pore size were produced and coated with a chitosan hydrogel (**Figure 6**). Mechanical testing evidenced that the maximum values of tensile and compressive strength were obtained by adding CaSH at 20% w/w concentration to the PHBV polymeric matrix. Moreover, biological tests were conducted both in vitro and in vivo, demonstrating that the CaSH and hydrogel addition improved the biocompatibility and osteogenic potential of the scaffolds.[208] A similar study on scaffolds for bone tissue engineering was recently conducted using PHBV and 45S5 BG particles.[209] Filaments were again produced by mechanical mixing (4% w/w BG content) and extrusion at 190 °C. However, in order to improve the adhesion between the filler and the polymer matrix, which is a known problem evidenced by many authors,[90,152,153] this group coated the BG by immersion in a 10% w/v solution of chlorotrimethylsilane (CTMS) in toluene. This resulted in more elastic filaments than the ones obtained with untreated BG particles, which were too brittle to be printed with traditional FDM machines. The scaffolds produced with this filament showed a good in vitro cytocompatibility and production of HA after immersion in simulated body fluid (SBF). Nevertheless, to obtain a better fibroblast interaction and adhesion, a direct coating of the scaffold with CTMS-treated BG proved necessary to better expose the bioactive particles on the surface.[209]

4.3. Thermoplastic Poly(ester urethane)s

All the previously mentioned thermoplastic polymers, despite being used in a broad variety of biomedical applications, are generally stiff materials. Therefore, they are mostly employed as substitutes for rigid (bone) or semirigid (cartilage) tissues. However, many tissues would require more flexible and ductile materials, while maintaining the positive characteristics of the analyzed polyesters. TPUs represent a valuable alternative in this regard, as their mechanical properties and degradability in biological environment can be tailored by selecting the building blocks accordingly.[210] In particular, the alternance between soft (generally the polyol component) and hard (diisocyanate and chain extender) segments creates a phase separation between crystalline and amorphous domains. Depending on the nature

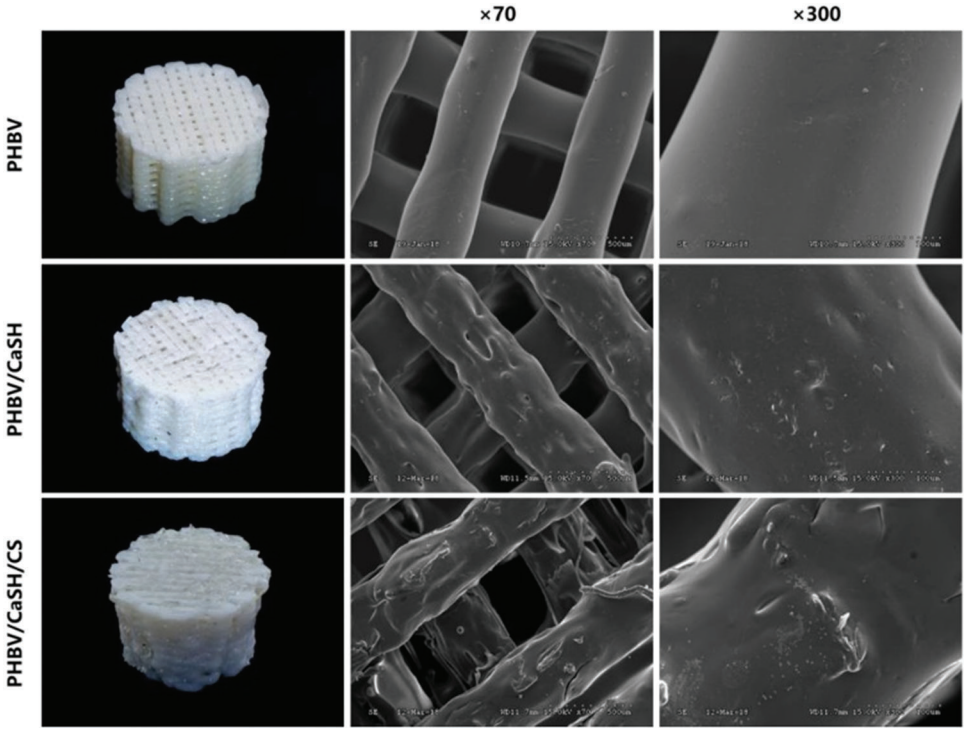

Figure 6. Scaffolds produced using PHBV and calcium sulfate hemihydrate (PHBV/CaSH) and coated with a chitosan hydrogel (PHBV/CaSH/CS) for bone tissue regeneration. Adapted with permission.[208] Copyright 2018, Elsevier.

of the constituents blocks, TPUs with a wide range of physicochemical properties can be obtained, spanning from stiff to highly elastomeric materials.[211–214] On the other hand, TPUs can be ad-hoc engineered to retain the typical processability of thermoplastics, making them suitable for FDM applications. Moreover, TPUs have already been used in biomedical applications to create implants, grafts, and also scaffolds for tissue engineering[215–219] and are known to be hemocompatible.[220]

Although either polycarbonates, polyethers or polyesters can form the polyol segment, for the scope of this review only the latter will be considered.

4.3.1. Custom-Made TPUs

Many groups have focused their research efforts on developing their own thermoplastic poly(ester urethane)s, combining the building blocks in order to obtain specific characteristics. Haryńska et al. published two different works in which they developed medical grade poly(urethane) filaments, given the current unavailability on the market of this kind of products.[210] In both cases, they used 1,6-hexamethylene diisocyanate (HDI) and 1,4-butanediol (BDO) as diisocyanate and chain extender, while the main difference resided in the polyol, which was either α,ω-dihydroxy (ethylene-butylene adipate) (PEBA)[221] or PCL.[210] From both materials, they obtained standard filaments for FDM (1.75 mm) in a temperature range between 170 and 200 °C. The effect of the isocyanate index (NCO:OH ratio) on the mechanical, thermal and physical properties was also investigated for the PCL-based polymer. When the index was higher (NCO:OH 1.1:1), the resulting material was more hydrophobic and the thermal stability increased, but a better cell compatibility was found for a lower index (0.9:1).[210] Biocompatibility and hemocompatibility were verified also for the PEBA-based poly(urethane) and its mechanical properties were comparable to commercial medical-grade TPUs.[221] Similarly, in a recent study Lores et al.[222] synthesized poly(urethane)s based on PCL, HDI, and BDO with different molar ratio between the three components, in order to obtain a high hard phase (HS) content (50–70% w/w). The aim was to develop materials with better elastomeric properties and higher elastic modulus, similar to commercial materials used for the production of scaffolds for articular cartilage repair.[223,224] It was found that an HS content >60% w/w did not permit to create homogeneous filaments due to thermal instability, while for a lower HS percentage good results were obtained in terms of filament production and printing performances. Indeed, the porous fabricated cylindrical structures exhibited mechanical properties compatible with cartilage tissue engineering applications.[222]

Among the polyols used for the synthesis of thermoplastic poly(ester urethane)s, PCL is by far the most diffused. Kiziltay et al.[220] synthesized a TPU based on PCL and L-lysine diisocyanate and produced scaffolds for bone regeneration using both FDM (printing temperature 105 °C) and a traditional salt leaching technique. Printed structures presented better osteoblast attachment and proliferation due to larger and more interconnected pores, although the overall porosity was higher for salt leached constructs (85–96% vs. 56–65% for the printed structures). Moreover, mineral matrix deposition was observed after 3 and 5 weeks, with an increase of Young's modulus up to 10%.[220] Also Chiono et al.[225] developed a PCL and

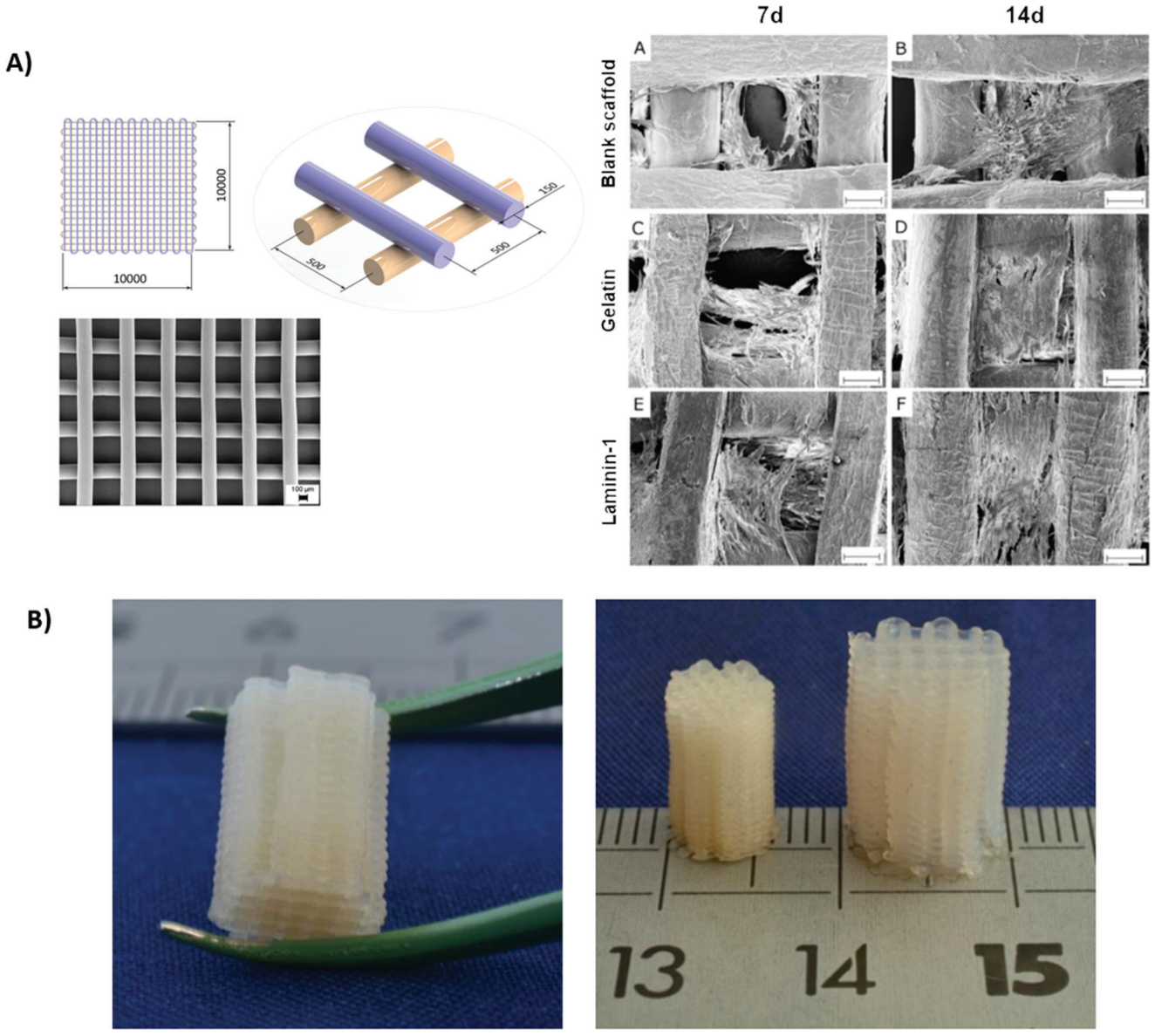

Figure 7. Examples of structures based on custom-made TPUs. A) Design of PCL-based TPU-printed scaffolds (left) and SEM images of human CPCs cultured on the scaffolds (TPU-printed structs as such and upon surface functionalization with gelatin or laminin-1) for 7 and 14 days. Scale bar: 100 μm. Reproduced under terms of the CC-BY license.[226] Copyright 2018, The Authors, Published by Public Library of Science. B) PEG-PCL-PEG-based TPU structures (left), before and after water absorption (right). Reproduced under terms of the CC-BY license.[227] Copyright 2018, The Authors, Published by MDPI.

lysine-based PU, using L-lysine ethyl ester as chain extender and 1,4-butandiisocyanate. The result was an elastomeric polymer that was successfully employed to produce scaffolds (printing temperature 155 °C) for cardiac tissue engineering. However, long-term proliferation of cardiac progenitors cells (CPCs) could not be supported without further scaffold functionalization.[225] To solve this issue, gelatin and laminin-1 were grafted on the scaffold surfaces using carbodiimide chemistry, after a surface plasma treatment with acrylic acid to expose carboxyl groups. CPC adhesion was highly improved, especially in the case of laminin-1 grafted samples, and also proliferation and differentiation toward cardiomyocytes, endothelial and smooth-muscle cells were reported (**Figure 7**A).[226] Finally, Güney et al.[227] improved TPU wettability using a polyol composed by PEG and PCL as building blocks for polymer synthesis. The hydrophilicity was modulated by incorporating different percentages of PEG into TPU backbone, while the use of PCL and relatively high molecular weight polyols (PEG–PCL–PEG starting copolymer with $\overline{M_n}$ around 20 000 Da) ensured adequate mechanical properties. The obtained structures (printing temperature 180 °C) were able to uptake a large quantity of water, up to 500% of the initial weight (Figure 7B). However, polyurethanes containing 70% of PEG in molar terms dissolved rapidly in water and therefore were not suitable for scaffold production.[227]

4.3.2. Commercial TPUs

Thermoplastic poly(urethane)s are also available in commercial and ready-to use filaments, although no medical-grade products are currently available on the market,[210,221] making the transition toward clinical application more difficult. However, despite their lower versatility, the use of commercial filaments significantly decreases costs since they can be processed by common 3D printers without further optimizations. This is particularly attractive for those applications that do not have too strong requirements in biological terms, such as surgical models or actuators.[140,228–230]

Surgical and preoperative models are important tools for surgeons. They require to be economical and fast to produce while maintaining accuracy to the patient anatomy. Generic FDM printers have affordable prices (few thousands of euros or dollars) and commercial filaments are significantly cheaper than custom-made ones. Chung et al.[228] used an ester-based commercial TPU (Ninjatek Cheeta) to print an abdominal aortic aneurism model, based on CT images taken from patients. Good transparency was obtained by printing at high temperature (255 °C) and with a 100% infill, although horizontal lines due to the layer deposition were still visible. Good flexibility and tear resistance (83 kN) were achieved, allowing an easy positioning of stents during surgical trials. Fabrication time (about 25 h) and cost (few euros) for each model were significantly lower than traditionally manufactured ones.[228] Similarly, Faletti et al.[229] designed a 3D printed aortic annulus model based on CT scans to facilitate measurements for aortic valve replacements, using a TPU similar to the previous one (Ninjatek Ninjaflex). They were able to produce a life-sized model with the appropriate accuracy for the required application in less than 20 min and with a cost of about 1€ (**Figure 8**A). An elastic modulus of 12 MPa and 1.2 mm thickness successfully represented the physiological conditions of the aortic annulus.[229]

The use of commercial materials does not prevent the possibility to add active agents or bioactive molecules; in this case, the TPU is purchased in form of pellets that can be mixed with the biomolecule and then extruded into a filament. For instance, drug-loaded meshes were produced to treat pelvic organ prolapse using Elastollan 80A TPU (BASF).[231] Different percentages of levofloxacin (LFX, 0.25–1% w/w), an antibacterial drug, were mixed to the TPU and 2.85 mm filaments were produced and then printed at 190 °C to obtain the final meshes (Figure 8B). The drug was partially retained inside the filaments due to entanglement phenomena with the polymer, so that the maximum release was found for 0.5% w/w LFX content; drug delivery was sustained for 3 days and an antibacterial activity was present. These meshes also presented lower stiffness (0.4 N mm^{-1}) than traditional poly(propylene) ones (2–6 N mm^{-1}).[231] Haryńska et al.[232] also produced filaments starting from commercial TPU pellets to be used for FFF scaffolds and demonstrated that filament production respecting standard requirements did not significantly alter the TPU characteristics. The filaments were then used to produce scaffolds with a pore pattern mimicking cancellous bone: after 28 days of incubation in SBF, the deposition of hydroxyapatite on the surface could be observed, thus demonstrating their bioactivity. The mechanical properties of the incubated scaffolds (Young's modulus around 0.2 GPa, tensile strength around 30 MPa, compression strength around 1.1 MPa) were also in the range of the native bone characteristics, making them promising for bone tissue engineering applications.[232]

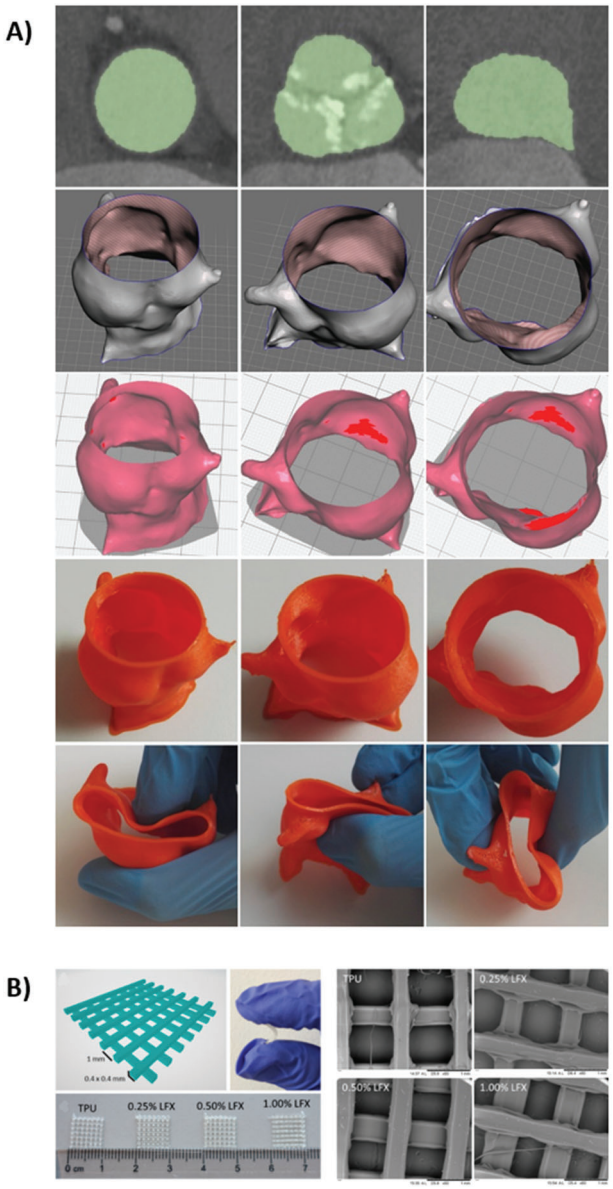

Figure 8. Application of commercial TPUs. A) Aortic annulus model obtained by FDM using Ninjatek Ninjaflex. Reproduced with permission.[229] Copyright 2018, Elsevier. B) Meshes made of Elastollan 80A TPU and loaded with different percentages of levofloxacin (LFX, 0.25–0.50–1% w/w) for pelvic prolapse treatment. Reproduced under terms of the CC-BY license.[231] Copyright 2020, The Authors, Published by MDPI.

TPUs are also valuable materials in the field of sensors and actuators. Evans et al.[140] incorporated MOFs not only in the previously mentioned PLA filaments, but also in a Semiflex (Ninjatek) TPU. In this case, a more complex production process was needed than with PLA, because MOFs did not maintain their electrochemical properties after loading into the pure TPU. The addition of poly(vinylidene fluoride-*co*-hexafluoropropylene) (PVDF-HFP) resulted in a tertiary complex able to create a more porous

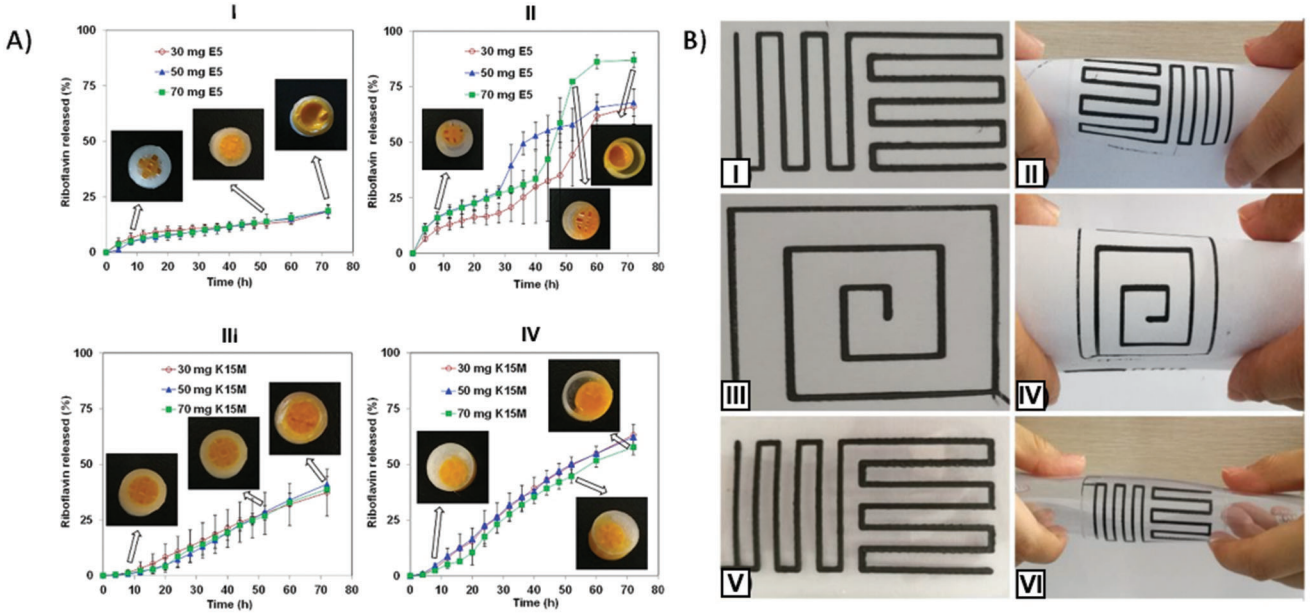

Figure 9. PLA-blends processed through FDM. A) Release profile of riboflavin from tablets made of a PLA/PCL blend and protected by a PLA cage for delivery through the gastric system. Different cage designs (presence of single (I–III) or double (II–IV) net), and tablet compositions (presence of 30–50–70 mg of hydroxypropyl methylcellulose, HPMC, type E5 (I–II) or K15M (III–IV)) are compared. Adapted with permission.[236] Copyright 2018, Elsevier. B) PLA/TPU blend with carbon-derived fillers used to obtain conductive and adhesive structures. Images show structures printed on paper (I–III) and on a flexible material (V) and their resistance to bending (II–IV–VI). Reproduced under terms of the CC-BY license.[241] Copyright 2019, The Authors, Published by MDPI.

structure exhibiting the proper sensing properties.[140] In case of actuators, Ninjaflex elasticity and flexibility were exploited to create a soft robot with reconfigurable, inflatable modules. The TPU spine to which the modules were attached permitted a wide range of positions and a fully controllable positioning of the robot.[230]

5. Polyester-Based Blends

The process of blending polymers is a widely used technique to improve the characteristics of the single materials. The combination of different polyesters is also common, although in many cases the polymers do not form miscible blends. Nevertheless, it is possible to form compatible mixtures by using coupling agents and adequate process parameters.[59] The main objective of blending is to combine the positive qualities of the polymers (elasticity, biocompatibility) while surmounting their limitations (brittleness, mechanical weakness). PLA and PCL are common blend bases and many examples of their combination with other polyesters such as PLGA, PHAs, and TPUs are present in the literature.[233–235]

Matta et al.[235] developed PLA blends with different PCL degrees (10%, 20%, 30% w/w) by melt blending at 170 °C and studied their mechanical and rheological properties. The blends resulted to be immiscible since two melting temperatures were present; however, PCL was well dispersed in the PLA matrix, although at 30% w/w concentration it formed large crystals that could facilitate creep formation. PCL was found to raise the blend elasticity and viscosity and interestingly its addition to PLA improved processability. The blends indeed showed a shear thinning behavior, favorable for printing applications. A PLA:PCL 8:2 blend was developed by Fu et al.[236] and used in combination with riboflavin and NaCl to obtain filaments for personalized drug delivery tablets (printing temperature 195 °C). A PLA cage with different configurations (single or double nets for riboflavin release) was also printed to further protect the tablets in the strongly acidic environment of the stomach. Results showed that the floating time in the digestive system, normally around 6–8 hours, could be prolonged to several days (3 days in an in vivo model). Moreover, the drug release could be modulated by varying the polymeric composition of the tablets and the cage (**Figure 9**A), in particular by adding hydroxypropyl methylcellulose (HPMC) of two different types, E5 and K15M, and in different amounts (30/50/70 mg) to the tablet formulation. In another study,[237] PLA and PCL were blended at 50:50 weight ratio to obtain scaffolds for bone tissue engineering. Scaffolds based on CT scans and printed with this material showed mechanical properties in the range of natural bone (compressive modulus in the range 59–159 MPa, depending on HA addition) and supported the proliferation of osteosarcoma cells immersed in a methacryloyl gelatin (GelMA) hydrogel for at least 5 days. An interesting characteristic of PLA/PCL blends that has been recently investigated by Liu et al.[238] is the thermoresponsive shape memory effect (SME). While the shape fixity was higher than 95% for all the tested blends (PCL range 10–60% w/w), they discovered that the SME was dependent on the blend composition and different printing parameters: in particular, high percentage of PCL, smaller layer thickness and symmetrical raster angles permitted a better shape recovery of the final structure. Final results indicated 50:50 PLA:PCL as the most promising blend formulation to obtain shape memory polymers and achieve a deformation

temperature near to PCL T_m and PLA T_g.[238] An alternative way to combine PLA and PCL properties without creating a "real" blend was also described.[239] The two polymers were not blended before printing, but they were alternatively deposited layer-by-layer to microfabricate a stent, using a double cartridge apparatus and a printing temperature of 200 °C. The final structure presented the typical characteristics of both polymers, exhibiting PCL elasticity when the stent expanded radially and PLA rigidity during recoil.

Blends of PLA and TPU are also reported. Guo et al. published two different works[240,241] in which they analyzed 70:20 PLA:TPU (commercial, Elastollan 85A) blends loaded with carbon-derived fillers (the remaining 10%), such as nanographite, graphene oxide (rGO) and carbon nanotubes. The integration with fillers did not affect the flexibility of the printed patterns, which could be easily incorporated onto other soft structures (Figure 9B), and TPU had a general strengthening effect on PLA. rGO as a filler also affected the thermal stability of the matrix; however, the same printing temperature of 210 °C used for PLA without fillers[240] was maintained. Nevertheless, the most important result regarded the electrical properties: resistivity could be brought to 10^3 Ω m, which is 9 orders of magnitude lower than the material without fillers. Hence, the printed structures showed high conductivity levels.[240,241]

5.1. PHA-Based Blends

Recently, several studies have focused on the design of blend systems for FDM applications based on PLA and PHAs, especially PHB. The aim is generally to lower the crystallinity degree of PLA, thus improving mechanical strength and elasticity.[242–244] Although the same goal could be reached by using other polyesters and fillers, PHAs are quite attractive because of their "green" nature. At the same time, the use of PHAs avoids the thermal limitations of other natural polymers that make them unsuitable for FDM applications. On the other hand, PHAs alone, especially those with a short side chain length, are not suitable for printing applications, since the filaments tend to shrink and twist on themselves.[242] Although both PLA and PHAs are mostly crystalline, during the blending process the crystallization on both parts is impaired, with the final effect to obtain a more amorphous material.[245,246] Despite these promising assumptions, studies on these blends in the biomedical field are very recent and mostly on an early stage.

Wang et al.[247] produced blends with different PLA/PHB weight ratios, ranging from 20/80 to 80/20, and then obtained filaments for FDM and studied their thermal and mechanical properties. The presence of PHB permitted to print the blends at a lower temperature (190 °C) than pure PLA (210 °C), due to a decrease in the flow index values. However, PHB could be added at a maximum concentration of 60% w/w to maintain good printing quality. Better results also in terms of mechanical properties (elongation at break) were found for 80/20 PLA/PHB blends.[247] Ecker et al.[248] used the same PLA/PHA ratio, but they employed a proprietary PHA copolymer instead of PHB. They compared the blend performance when processed with injection molding and FDM; in general, PLA/PHA 3D printed parts reached better results than traditional and pure PLA scaffolds, with 90% higher impact strength values. This behavior can be explained by the more stable crystalline structure that was formed by the blends. Moreover, pure PLA presented lower values of tensile strength than blends, regardless of the processing method, and this is probably due to the presence of the amorphous PHA.[248] Although these two studies showed fairly good results, Menčík et al. have highlighted that PLA/PHA blends remain brittle and tend to thermally degrade at conditions near the printing temperatures;[249] thus, the effect of plasticizers was investigated to improve the printability of these blends. The plasticizers investigated in this study belong to the Citroflex family and are derived from citric acid esters; furthermore, this study was focused on blends in which PHB was the main component, while usually the PLA/PHA ratio is in favor of PLA. The final percentages used to prepare FDM filaments were 60% w/w for PHB, 25% w/w for PLA, and 15% w/w for the plasticizer. The two smallest monomers tested within the Citroflex family (i.e., tributyl citrate and acetyl tributyl citrate) showed the best plasticizing effects on 3D printed dog-bone structures, with an improvement of elongation at break up to 300% and a T_g more than 30 °C lower than pure PLA.[249]

Some PLA/PHA-based filaments for FDM applications are also commercially available. In particular, ColorFabb filaments, containing ≈88% of PLA, have been studied by several groups.[244,250,251] The majority of them evaluated the effect of the printing parameters, especially temperature, on the blend properties.[250] Thermal degradation was detected at 260 °C, while poor printing quality was observed at 190 °C, although this temperature is comprised in the processing range reported by the manufacturer (190—210 °C). Compared to PLA, the mechanical strength was reduced, but elongation at break was 40 times higher, in accordance to what was reported elsewhere for blends with a PLA content higher than PHA.[247,248] A ductility improvement was found by processing the material at 210 °C.[250] Accordingly, Guessasma et al. reported that an acceptable processability range could be between 210 and 255 °C. Printing at higher temperatures also required a longer cooling time, that was found to produce lower crystallinity degrees and therefore more ductile structures.[244] Gonzales Ausejo et al.,[251] on the other hand, investigated the effect of the printing direction on the mechanical and degradation properties of ColorFabb. They printed dog-bone samples both horizontally and vertically; the vertical-printed structures showed greater crystallization and therefore higher mechanical strength, but horizontal-printed ones had a better resistance to degradation. The vertical structure was completely pulverized after 70 days at 50 °C, while the horizontal samples were still present even if not completely intact. They also tested the cytotoxicity of this material toward human embryonic kidney cells and no negative effects were reported.[251]

Although PHAs are usually blended with PLA, a PHBV/PCL blend has also been developed for tissue engineering purposes.[252] Different mixtures were created (PCL/PHBV 25/75, 50/50, and 75/25) and scaffolds were produced at 160–170 °C by overlapping layers with a 45° angular shift (**Figure 10**). The compressive strength value increased with the PHBV content by threefold compared to pure PCL scaffolds. Additionally, an O_2 plasma treatment significantly improved hydrophilicity and surface roughness (from ≈40 to ≈100 nm for the formulation with the highest PHBV content). In this way, chondrocytes were

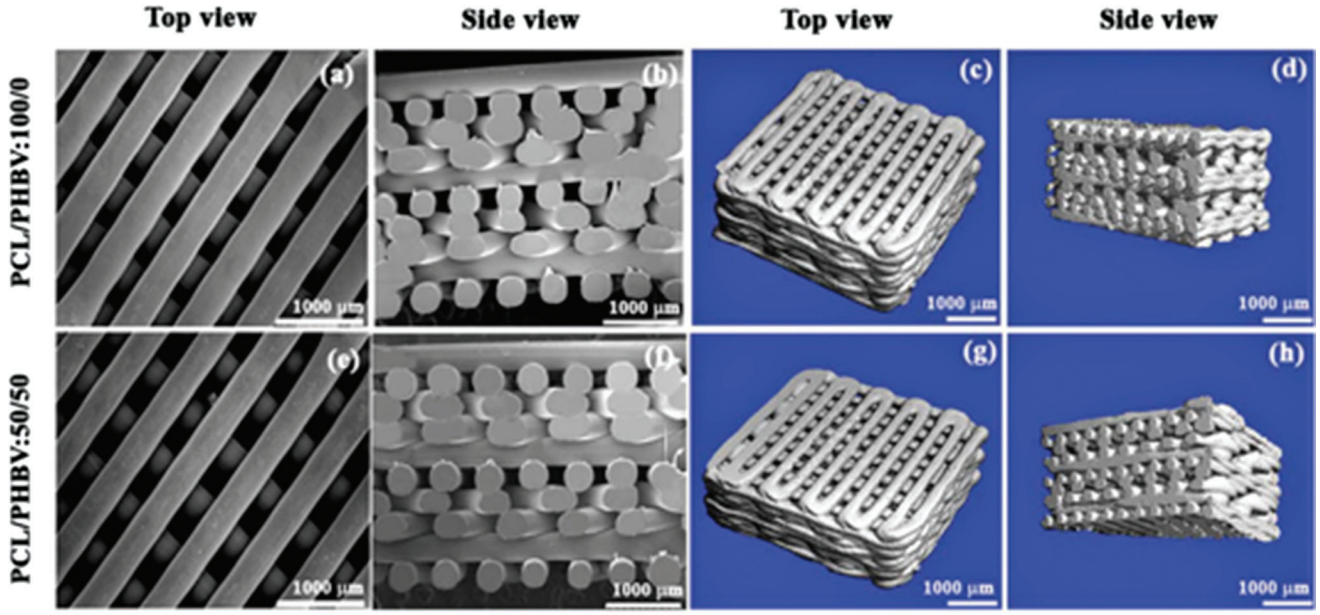

Figure 10. PCL/PHBV blend-based constructs for cartilage regeneration. Comparison between a–d) pure PCL-based and e–h) 50:50 PCL:PHBV blend-based scaffolds. Reproduced with permission.[252] Copyright 2017, Wiley Periodicals LLC.

able to proliferate on the scaffold surface, making this structure suitable for cartilage repair.[252] In a more recent study, the same group worked on further improving the surface hydrophilicity of these scaffolds by immersing them in a NaOH solution (1 M) for 150 min at 60 °C. Moreover, NaOH particles were added during filament production, so that additional small pores (1–5 μm) could be created by salt leaching on the final FDM printed structures. These modification resulted in immediate absorption of liquids from the scaffold surface, accelerated degradation and higher chondrocyte proliferation rates and glycosaminoglycan (GAG) production compared to the unmodified structures.[253]

5.2. PLGA/PCL Blends

As previously mentioned, PLGA is not widely used in FDM applications due to its tendency to easily undergo thermal degradation. However, blending PLGA with other polymers, including polyesters, can be a promising approach to overcome its limitations. For instance, several research groups have mixed this copolymer with PCL. Kim and Cho[17] produced 50/50 PLGA/PCL blends by melting the two polymers together at 90 °C; the mixture was then printed at 120 °C to obtain rectangular scaffolds with a grid-like structure. Porosity was around 70% and compressive modulus and strength reached values of 12.9 and 0.8 MPa, respectively. Moreover, mesenchymal cells were successfully cultured on these structures and proliferated up to 15 days.[17] In a following study by the same group,[23] different PLGA/PCL blends (25/75, 50/50, and 75/25) were analyzed and compared to pristine PCL and PLGA. Printing temperature and pressure varied by changing the blend formulation within the ranges 95–115 °C and 450–650 kPa, respectively. The compressive modulus of the printed structs was significantly reduced by increasing the PLGA content in the blends, even if all the scaffolds retained their shape and mechanical stability during the biocompatibility tests. All fabricated structures supported mesenchymal stem cell proliferation, but the best compromise between mechanical properties and biocompatibility was identified in the PCL/PLGA 75/25 blend.[23]

The typical target for PLGA/PCL scaffolds is bone tissue engineering. The addition of PLGA to PCL can improve its stiffness, which is important when developing bone substitutes, and also lower its hydrophobicity, promoting cell adhesion as previously demonstrated.[17,23] However, to improve osteogenesis and compatibility with the native bone tissue, other cues are generally incorporated. For instance, TCP was employed in two different studies. Idaszek et al.[254] studied ternary composites containing different quantities of PCL, PLGA, and TCP. With a 5% w/w addition of TCP, the Young's modulus increased over 30%, but when PLGA quantities above 15% w/w were added, the cumulative stress on the PCL matrix resulted in worse mechanical properties. PLGA and TCP improved surface wettability (contact angle around 65° compared to 80° for pure PCL) and degradation. This aspect influenced cell attachment and proliferation, which was more favorable for ternary composites with 70% w/w PCL, 25% w/w PLGA, and 5% w/w TCP after 7 days. A similar ternary system was developed by Shim et al.,[147] that first blended PCL and PLGA at a 50:50 ratio, and then added TCP to reach a concentration of 20% w/w in the final composite. They produced scaffolds with a compressive modulus around 50 MPa, which is comparable to the native cancellous bone. In vivo implantation in a rabbit cranium defect showed that after 8 weeks the PCL/PLGA/TCP scaffolds were able to promote new tissue formation, thanks to an optimized degradation rate, with a tissue development greater than when no scaffold was implanted.[147]

Another strategy employed to increase PCL/PLGA scaffold biocompatibility is surface modification. Two different studies exploited mussel-inspired coatings to graft bioactive molecules

on the scaffold surfaces. In the first study,[255] a previously optimized PLGA/PCL 50/50 scaffold[16] was surface functionalized by immersing the structure in a solution of mussel adhesive protein (MAP) fp-151 modified with an arginine-glycine-aspartic acid (RGD) peptide. Effects of this functionalization were visible in vitro, with a good proliferation of adipose-derived stem cells, while in vivo good bone regeneration and no inflammation response were detected on a calvarial defect in a rabbit model. On the other hand, in the study by Kim et al.,[256] PCL and PLGA were blended at an equal ratio, and printed at 130 °C according to a CAD design that matched a defect in a rat tibia. The scaffold was then coated with a negatively charged heparin–dopamine conjugate (Hep–DOPA), which was used to immobilize the positively charged BMP-2 on the surface. The in vitro delivery study presented a burst release after 1 day, due to the low electrostatic interactions between heparin and BMP-2, followed by a sustained release for at least one month. Osteoblast-like differentiation was supported in vitro and new bone formation was observed in vivo after 8 weeks of implantation.[256]

6. Discussion and Future Perspectives

The employment of biodegradable thermoplastic polyesters in 3D printing applications has gained a growing interest in the biomedical field, especially over the last decade. In particular, fused deposition modeling, which is one of the most diffused and easy to handle rapid prototyping techniques, has been thoroughly investigated. A recap of the studies found in the literature and discussed in this review is reported in **Table 2** for tissue engineering applications and **Table 3** for other biomedical applications.

For medical applications, the possibility to obtain highly personalized products in a cost-effective manner is crucial. 3D printing methods are particularly advantageous in this sense, since the printed structure can be modeled directly on the patient anatomy with an accuracy that is impossible or very difficult to achieve with traditional manufacturing processes. Also the microarchitecture of the products can be tailored with a higher degree of precision, so that pore dimension and shape can be adapted to the different human tissues' requirements. However, the accuracy and resolution that can be achieved by traditional FDM techniques can be limited in this sense. The relevant dimensional errors often evidenced (±0.1 mm) can be particularly detrimental for tissue engineering applications, in which pore dimension and filament diameter requirements are usually in this same dimensional range.[9] So, further work is needed to improve both the FDM technology and the material performances in matching the desired scaffold architecture and properties.

As discussed at the beginning of this review, several process and material parameters need to be considered when an FDM produced part is designed and many issues still need to be overcome. One of the drawbacks that affects FDM use in industry is the anisotropy of the manufactured parts, mostly due to a weakness given by the not perfect adherence between layers. However, as most human tissues are by nature anisotropic, if the FDM manufacturing process is correctly designed, this inherent disadvantage can become an asset to better mimic the complex architecture of biological tissues. Different raster angles, infill densities and layer thicknesses have been extensively explored and the influence of the internal structure of scaffolds on the mechanical properties is actually one of the most investigated themes in the literature. Nevertheless, most studies are still centered on simple and linear geometries that are a simplistic representation of the complexity of natural tissues. Only in recent years, some groups have tried to exploit FDM versatility by studying more complex geometries, both at the macroscopic and microscopic level, to better represent tissues also in a personalized scenario. Although results obtained using this approach are not always better than the ones found for simpler constructs, research in this sense is certainly needed in order to use CAD design and FDM at their maximum potential in the tissue engineering field.

Another area of application for which FDM and 3D printing in general will be highly beneficial is organ and tissue modeling. This sector has seen an increasing interest in the last years, especially due to ethical issues related to the use of animals in research, with the developing of the 3Rs principle (replacement, reduction, and refinement) and its implementation in many countries legislations. Tissue and organ models are particularly relevant for drug screening and toxicology testing purposes, for which the animal model can sometimes not be perfectly representative of the human response.[257] However, standardized in silico devices and protocols would be needed to obtain reliable results and completely overcome the need of living animal models. Organs-on-chip are currently seen as the new frontier in the field and they heavily rely on 3D printing in general for their implementation, since they usually combine bioprinting with more classical techniques such as FDM to reproduce and sustain all the complexity of a physiological system. Indeed, the easy scalability and customization of FDM techniques, combined with a relevant reduction in costs with respect to animals, represents a powerful tool to sustain in silico models in becoming the next gold standard in this field.

Polyesters are an important class of polymers commonly used for biomedical purposes. They possess thermoplastic properties that make them suitable for printing in a melt state, as in FDM applications. The ester group is also susceptible to hydrolysis and enzymatic activity (e.g., by lipase enzymes), so many of these materials are also biodegradable after implantation, albeit generally in a quite long time (some years). In general, the polyesters reviewed in this paper degrade in vivo in a period ranging from ≈1 to 6 years, depending on the single polymer characteristics and the manufacturing processes. Moreover, their degradation products are not toxic and can also be substances normally found in the body (e.g., lactic acid for PLA). Given their long surviving time in the body and the mechanical properties shared by these materials, hard tissues are the typical target for their use in tissue engineering. Bone regeneration is the most studied application since thermoplastic polyesters offer a primary stability comparable to the native tissue and a degradation rate able to match the natural regrowth. Despite all these positive characteristics, it is usually necessary to modify the starting polymer to overcome some limitations, such as hydrophobicity or excessive brittleness. The strategies employed in the literature are various and range from the use of fillers and additives to obtain composites, to the development of blend polymeric systems. Although the mechanical properties can be greatly improved using these methods, researchers should also consider their effects on the thermal response and stability of the polymers, which are fundamental parameters to consider for FDM applications.

Table 2. Summary of polyesters uses in FDM for tissue engineering applications (n.r. = not reported).

Application	Material	Printing temperature [°C]	Pore size	Additive(s) [% w/w]	Functionalization(s) and/or cell loading	In vitro/ in vivo study
Bone tissue engineering applications	PCL[71]	120	200–300 μm	None	Gelatin; fibronectin	In vitro
	PCL[72]	140	0.4–4.5 mm^2	None	BMP-2 and BMP-7 in PLGA/PHBV nanocapsules	In vivo
	PCL[73]	100	120 × 170 μm (ellipse)	None	Hyaluronic acid; methacrylated collagen	In vitro
	PCL[76]	70–120	800 μm	None	None	Both
	PCL[74]	>100	250–300 μm	None	PRP	Both
	PCL[80]	160	n.r.	β-TCP (20/40/60%)	None	In vitro
	PCL[81]	n.r.	515 μm/n.r.	β-TCP/BCP (20%)	None	In vivo
	PCL[27]	n.r.	515 μm	β-TCP (20%)	Fibrin-immersed MSCs	Both
	PCL[83]	n.r.	515 μm	β-TCP (20%)	MSCs	In vivo
	PCL[85]	100	765 ± 83 μm/746 ± 71 μm	HA (30%)	None	Both
	PCL[87]	85	>600 μm	None	β-cyclodextrin grafted HA; Simvastasin	Both
	PCL[89]	100	<2 mm	SrBG, 45S5 (10%)	None	In vitro
	PCL[90]	90	<2 mm	SrBG, 45S5 (50%)	CaP	Both
	PCL[91]	n.r.	372.3 ± 10.7 μm	BG, 58S (5–20%)	None	Both
	PCL[92]	80	800 μm	DBM (5/30/70/85%)	hADSCs	Both
	PCL[93]	80	390 μm	None	ECM produced in situ by MSCs	In vitro
	PLA[148]	186	150–250 μm	None	None	In vitro
	PLA[150]	210	300 μm	HA (10%)	None	Both
	PLA[146]	n.r.	800–1800 μm	None	Polydopamine; BMP-2	In vitro
	PLA[151]	n.r.	n.r.	BG, 45S5	None	In vitro
	PLA[152]	110–145	0.5625 mm^2	BG, 45S5 (1–10%)	None	In vitro
	PLA[28]	205	400–600 μm	None	None	None
	PLA[156]	210	300–600 μm	HA (5/10/15%)	None	None
	PLA[158]	n.r.	Not porous	None	None	In vitro
	PLGA[196]	85	n.r.	β-TCP (25%)	HA	In vivo
	PHBV[208]	n.r.	400 μm	CaSH (5–30%)	Chitosan	Both
	PHBV[209]	196	4.76–0.04 mm^2	CMTS-coated BG, 45S5 (4%)	CMTS-coated BG, 45S5	In vitro
	PCL-based TPU[220]	105	80–488 μm	None	None	In vitro
	Commercial TPU[232]	210	n.r.	None	None	In vitro
	PLA:PCL 50:50[237]	160	n.r.	None	GelMA	In vitro
	PLGA:PCL (5–25% PLGA)[254]	95–105	300–350 μm	β-TCP (5%)	None	In vitro
	PLGA:PCL 50:50[147]	135	300 μm	β-TCP (20%)	None	In vivo
	PLGA:PCL 50:50[255]	130	300 μm	None	RGD-modified MAP fp-151	Both
	PLGA:PCL 50:50[256]	130	n.r.	None	Heparin-dopamine; BMP-2	Both
Cartilage tissue engineering applications	PCL[103]	110	n.r.	None	None	None
	PCL[104]	120	800 μm	HA (30%)	UCB-MSCs/chondrocytes	Both
	PCL[106]	60	100–150 μm	HA (40%)	Methacrylated hyaluronic acid; TGF-β_1	In vivo
	PCL[107]	100	<100 μm	None	Methacrylated gellan gum hydrogel	In vitro

(*Continued*)

Table 2. (Continued).

Application	Material	Printing temperature [°C]	Pore size	Additive(s) [% w/w]	Functionalization(s) and/or cell loading	In vitro/ in vivo study
	PCL[105]	130	303.3 ± 32.7 μm	None	PLGA–PEG–PLGA thermogel	In vitro
	PLGA[194]	170	1.15 mm	None	Collagen type II	In vitro
	PCL-based TPU[222]	165–180	130–900 μm	None	None	In vitro
	PHBV:PCL 25:75/50:50/75:25[252]	160–170	n.r.	None	None	In vitro
	PHBV:PCL 25:75/50:50/75:25[253]	80–150	200–400 μm	None	None	In vitro
Dental substitutes	PCL[96]	130	300 μm	β-TCP (50/70%)	None	In vitro
Periodontium reconstruction	PCL[100]	120	200 μm	HA (20%)	SDF1- and BMP-7-loaded collagen	In vivo
	PCL[97]	n.r.	515 μm	β-TCP (20%)	Calcium phosphate; osteoblasts; PL cell sheets	Both
	PCL[98]	120	100/300/600 μm	HA (10%)	PLGA μparticles containing amelogenin/CTGF/ BMP-2; DPSCs	In vitro
Cardiac tissue engineering applications	PCL-based TPU[225,226]	155	500 ± 4 μm	None	Gelatin, Laminin-1	Both
Trachea reconstruction	PCL[24]	100–130	300 μm	None	Fibrin-immersed MSCs	Both
	PCL[113]	140	<200 μm	None	None	Both
Ear substitute	PCL[108]	85	n.r.	None	Fibrin/hyaluronic acid hydrogel	In vitro

For example, despite the presence in the literature of several successful studies on the use of fillers or additives in FDM filament production, a thorough investigation of their dispersity inside the polymeric matrix should be performed. Indeed, it has been observed that particles can be isolated from the filament surface because of the presence of a plastic skin around them, thus preventing their bioactivity.[258] A possible solution to this problem is alkaline erosion of the final scaffold surface to better expose the bioactive agent;[259,260] still, this process adds a further step in the device production that increases the degree of complexity of the entire fabrication pipeline and also damages the structural stability if not correctly controlled.

As also noted elsewhere,[42] when moving from traditional techniques to additive manufacturing, it is important to take into account the specific requirements of the printing process in the early stage of material development. Besides, in the specific case of FDM, the production of standard filaments to be used with commercial printers must be considered, since this is one of the crucial aspects to ensure the correct operation of the FDM machines. Hence, the thermal and mechanical effects of both the filament fabrication and the further melting process during extrusion need to be addressed. Indeed, the ability of polymers to withstand all the production steps affects the printing quality, which is fundamental to obtain good fidelity to the CAD model and thus ensure good reproducibility. At the current time, there is a lack of commercial materials that can be readily used to print structures for medical purposes. No optimized filaments that have also been approved by the regulatory agencies are indeed available; this is an important aspect to address to shorten the path between research and clinic. Moreover, also in the available studies there is a lack of a thorough chemical, thermal, and rheological characterization of the materials especially before the printing process.[37] Usually, also the finished parts are mostly characterized only in terms of mechanical strength and resistance. This severely limits the knowledge on the material behavior during the printing process that would instead be highly beneficial in the printing parameter settings. The current approach in this sense seems to be more of a "trial and error" type, with the optimization based on the repetition of the process until the desired characteristics are achieved in the final product.[42] Although this kind of methodology will always be needed, a deeper knowledge of the material properties and responses could be helpful in making the printing optimization a less time and material consuming process.

The use of 3D printing techniques and especially FDM thus present many interesting traits for tissue engineering and regenerative medicine. Nevertheless, there are still several issues that need to be confronted to fully exploit this technology in these fields. For this reason, although results are in many cases promising, all the studies presented in this review are still in the preclinical phase. For 3D printing techniques in general, there is a scarcity of clinical trials that have reached conclusions. Moreover, the available data on clinical trials are often affected by biases given by the limited number of patients.[261,262] For example, a clinical study involving an FDM-printed PCL scaffold for cleft alveolus reconstruction has been successfully conducted,[263] involving only one patient. Other limited examples can be found in the maxillo-facial and orthopedic fields,[264] but they usually involve other additive manufacturing techniques beside FDM. Conversely, some examples of FDM use in clinical practice can be found with drug delivery[117,265]

Table 3. Summary of polyesters uses in FDM for other biomedical applications (n.r. = not reported).

Application	Material	Printing temperature [°C]	Pore size	Additive(s) [% w/w]	Functionalization(s) and/or cell loading	In vitro/ in vivo study
Drug delivery systems	PCL[116]	140	400–600 μm	β-TCP (20%)	Fibrin/BMP-2	In vitro
	PCL[30]	53	Not porous	Quinine (2.5–25%)	None	None
	PLA[168]	195	Not porous	None	Methylene blue; fluorescein	In vitro
	PLA[169]	220	600 μm	Dexamethasone (1%)	Prednilosone	In vitro
	PLGA[197]	105	n.r.	mAb (15%)	None	In vitro
	PLA:PCL 80:20[236]	195	Not porous	None	Riboflavin; NaCl	Both
	PCL[117]	100	Not porous	Indomethacin (5/15/30%)	None	None
	PCL[115]	80	Not porous	None	None	In vitro
Surgical meshes	PCL[118]	n.r.	n.r.	β-TCP (20%); gentamicin sulfate (5/15/25%)	None	Both
	PCL[119]	120–130	≈800 μm	Barium-, iodinated-, gadolinium-containing contrast agents (10%)	None	In vivo
	Commercial TPU[231]	190	n.r.	LFX (0.25–1%)	None	In vitro
Surgical and anatomical models	PLA[170]	n.r.	Not porous	None	None	None
	Commercial TPU[228]	255	Not porous	None	None	None
	Commercial TPU[229]	230	Not porous	None	None	None
Surgical instruments	PLA[132]	240	Not porous	None	None	None
Vascular stent	PLA[157]	200	Not porous	None	None	None
Eluting catheters	PLA[167]	170–220	Not porous	Gentamicin sulphate (1%); methotrexate (2.5/5%)	None	In vitro
Sensors	PLA[182]	n.r.	Not porous	Graphene	None	In vitro
	PLA[181]	210	Not porous	Carbon black	None	In vitro

and especially surgical and preoperative models.[266–268] In this second case, the absence of strong biological requirements has simplified their introduction in the medical practice, also from a regulatory perspective, which on the other hand is one of the strongest hindrances for implantable devices.[269] As noted by many authors,[4,9,41] the current absence of a dedicated regulation for FDM parts, from the mechanical characterization to the suitability of the final struct or device for medical use, is severely damaging both the developer evaluation of its products before the marketing stage and the final step of legal acceptance and implementation among the biomedical products.

7. Conclusions

In this work, the use of thermoplastic polyesters in biomedical 3D printing has been comprehensively surveyed and analyzed, focusing on their application in fused deposition modeling. The advantages of this technique in the production of medical devices and scaffolds for tissue engineering purposes have been evidenced, considering especially the introduction and development of personalized and patient-specific approaches in the medical field. Many examples of successful literature studies reporting the processing of PCL, PLA, PLGA, PHAs, PUs, and their blends for the repair and regeneration of different tissues have been analyzed and reported in this review. At the same time, some issues concerning the application of this technology have been evidenced, regarding in particular the optimization of FDM in terms of accuracy and geometrical complexity, the lack of proper material characterization before processing and the difficulties on the translation from research to actual medical trials. The route toward a complete integration between additive manufacturing and clinical practice is thus still long, but the available background is quite solid and ever growing as long as research keeps expanding in this sense.

Acknowledgements

This work was developed in the framework of the ALTERNATIVE project, which was received funding from the European Union's Horizon 2020 research and innovation programme under Grant Agreement No. 101037090. The content of this publication reflects only the author's view and the Commission is not responsible for any use that may be made of the information it contains.

Open Access Funding provided by Politecnico di Torino within the CRUI-CARE Agreement.

Conflict of Interest

The authors declare no conflict of interest.

Keywords

3D printing, biomedical devices, fused deposition modeling, thermoplastic polyesters, tissue engineering

Received: January 29, 2022
Revised: April 11, 2022
Published online:

[1] C. K. Chua, K. F. Leong, *3D Printing and Additive Manufacturing: Principles and Applications, The 5th Edition of Rapid Prototyping: Principles and Applications*, World Scientific Publishing Company, Singapore **2017**.
[2] B. Berman, *Bus. Horiz.* **2012**, *55*, 155.
[3] A. Zadpoor, *Int. J. Mol. Sci.* **2017**, *18*, 1607.
[4] O. A. Mohamed, S. H. Masood, J. L. Bhowmik, *Adv. Manuf.* **2015**, *3*, 42.
[5] S. Cai, C. Wu, W. Yang, W. Liang, H. Yu, L. Liu, *Nanotechnol. Rev.* **2020**, *9*, 971.
[6] C. M. González-Henríquez, M. A. Sarabia-Vallejos, J. Rodriguez-Hernandez, *Prog. Polym. Sci.* **2019**, *94*, 57.
[7] J.-Y. Lee, J. An, C. K. Chua, *Appl. Mater. Today* **2017**, *7*, 120.
[8] J. R. C. Dizon, A. H. Espera, Q. Chen, R. C. Advincula, *Addit. Manuf.* **2018**, *20*, 44.
[9] T. N. A. T. Rahim, A. M. Abdullah, H. Md Akil, *Polym. Rev.* **2019**, *59*, 589.
[10] S. S. Crump, *ASME, PED* **1991**, *50*, 53.
[11] P. Minetola, M. Galati, *Addit. Manuf.* **2018**, *22*, 256.
[12] A. K. Sood, R. K. Ohdar, S. S. Mahapatra, *Mater. Des.* **2010**, *31*, 287.
[13] M. Srivastava, S. Rathee, S. Maheshwari, T. Kundra, *Additive Manufacturing: Fundamentals and Advancements*, CRC Press, Singapore **2019**.
[14] N. Volpato, D. Kretschek, J. A. Foggiatto, C. M. Gomez Da Silva Cruz, *Int. J. Adv. Manuf. Technol.* **2015**, *81*, 1519.
[15] F. Calignano, M. Galati, L. Iuliano, P. Minetola, *J. Healthcare Eng.* **2019**, *2019*, 9748212.
[16] J.-H. Shim, J. Y. Kim, J. K. Park, S. K. Hahn, J.-W. Rhie, S.-W. Kang, S.-H. Lee, D.-W. Cho, *J. Biomater. Sci., Polym. Ed.* **2010**, *21*, 1069.
[17] J. Y. Kim, D.-W. Cho, *Microelectron. Eng.* **2009**, *86*, 1447.
[18] M. Shunmugasundaram, A. A. B. Maughal, M. Ajay Kumar, *Mater. Today Proc.* **2020**, *27*, 1596.
[19] R. Nicot, G. Couly, J. Ferri, J.-M. Levaillant, *Int. J. Oral Maxillofac. Surg.* **2018**, *47*, 44.
[20] V. Bagaria, K. Chaudhary, *Injury* **2017**, *48*, 2501.
[21] I. Chiulan, A. N. Frone, C. Brandabur, D. M. Panaitescu, *Bioengineering* **2018**, *5*, 2.
[22] E. Carlier, S. Marquette, C. Peerboom, L. Denis, S. Benali, J.-M. Raquez, K. Amighi, J. Goole, *Int. J. Pharm.* **2019**, *565*, 367.
[23] M.-W. Sa, J. Y. Kim, *Int. J. Precis. Eng. Manuf.* **2013**, *14*, 649.
[24] J. W. Chang, S.u A. Park, J.u-K. Park, J. W. Choi, Y.-S. Kim, Y. S. Shin, C.-H. Kim, *Artif. Organs* **2014**, *38*, E95.
[25] D. S. Chan, N. Fnais, I. Ibrahim, S. J. Daniel, J. Manoukian, *Int. J. Pediatr. Otorhinolaryngol.* **2019**, *123*, 38.
[26] Y. Li, C. Liao, S. C. Tjong, *Nanomaterials* **2019**, *9*, 590.
[27] B. Rai, J. L. Lin, Z. X. H. Lim, R. E. Guldberg, D. W. Hutmacher, S. M. Cool, *Biomaterials* **2010**, *31*, 7960.
[28] R. Pecci, S. Baiguera, P. Ioppolo, R. Bedini, C. Del Gaudio, *J. Mech. Behav. Biomed. Mater.* **2020**, *103*, 103583.
[29] J. Long, H. Gholizadeh, J. Lu, C. Bunt, A. Seyfoddin, *Curr. Pharm. Des.* **2017**, *23*, 433.
[30] W. Kempin, C. Franz, L.-C. Koster, F. Schneider, M. Bogdahn, W. Weitschies, A. Seidlitz, *Eur. J. Pharm. Biopharm.* **2017**, *115*, 84.
[31] G.-H. Wu, S.-H. Hsu, *J. Med. Biol. Eng.* **2015**, *35*, 285.
[32] A. Salem Bala, S. Bin Wahab, M. Binti Ahmad, *Adv. Eng. Forum* **2016**, *16*, 33.
[33] O. A. Mohamed, S. H. Masood, J. L. Bhowmik, *Mater. Manuf. Process.* **2016**, *31*, 1983.
[34] D. Popescu, A. Zapciu, C. Amza, F. Baciu, R. Marinescu, *Polym. Test.* **2018**, *69*, 157.
[35] H. I. Medellin-Castillo, J. Zaragoza-Siqueiros, *Chin. J. Mech. Eng. (Engl. Ed.)* **2019**, *32*, 1.
[36] R. B. Kristiawan, F. Imaduddin, D. Ariawan, Ubaidillah, Z. Arifin, *Open Eng.* **2021**, *11*, 639.
[37] S. Vyavahare, S. Teraiya, D. Panghal, S. Kumar, *Rapid Prototyping J.* **2020**, *26*, 176.
[38] M. L. Dezaki, M. K. A. Mohd Ariffin, *Polymers* **2020**, *12*, 2792.
[39] D. Singh, R. Singh, K. S. Boparai, *J. Manuf. Process.* **2018**, *31*, 80.
[40] N. A. S. Mohd Pu'ad, R. H. Abdul Haq, H. Mohd Noh, H. Z. Abdullah, M. I. Idris, T. C. Lee, *Today Proc.* **2019**, *29*, 228.
[41] B. Thavornyutikarn, N. Chantarapanich, K. Sitthiseripratip, G. A. Thouas, Q. Chen, *Prog. Biomater.* **2014**, *3*, 61.
[42] A. Das, C. A. Chatham, J. J. Fallon, C. E. Zawaski, E. L. Gilmer, C. B. Williams, M. J. Bortner, *Addit. Manuf.* **2020**, *34*, 101218.
[43] M. E. Mackay, *J. Rheol.* **2018**, *62*, 1549.
[44] D. A. Roberson, C. M. Shemelya, E. MacDonald, R. B. Wicker, *Rapid Prototyp. J.* **2014**, *21*, 514.
[45] A. García-Domínguez, J. Claver, A. M. Camacho, M. A. Sebastián, *Materials* **2020**, *13*, 28.
[46] I. Buj-Corral, A. Bagheri, O. Petit-Rojo, *Materials* **2018**, *11*, 1532.
[47] S. Wang, L. Capoen, D. R. D'hooge, L. Cardon, *Plast., Rubber Compos.* **2018**, *47*, 9.
[48] V. Guarino, G. Gentile, L. Sorrentino, L. Ambrosio, *Encyclopedia of Polymer Science and Technology*, John Wiley & Sons, Inc., Hoboken, NJ, USA **2017**, pp. 1–36.
[49] J. N. Hoskins, S. M. Grayson, *Macromolecules* **2009**, *42*, 6406.
[50] M. A. Woodruff, D. W. Hutmacher, *Prog. Polym. Sci.* **2010**, *35*, 1217.
[51] E. Malikmammadov, T. E. Tanir, A. Kiziltay, V. Hasirci, N. Hasirci, *J. Biomater. Sci., Polym. Ed.* **2018**, *29*, 863.
[52] K. Schäler, A. Achilles, R. Bärenwald, C. Hackel, K. Saalwächter, *Macromolecules* **2013**, *46*, 7818.
[53] S.-H. Teoh, B.-T. Goh, J. Lim, *Tissue Eng., Part A* **2019**, *25*, 931.
[54] I. Zein, D. W. Hutmacher, K. C. Tan, S. H. Teoh, *Biomaterials* **2002**, *23*, 1169.
[55] M. Abedalwafa, L. Wang, F. Wang, C. Li, *Adv. Mater. Sci.* **2013**, *34*, 123.
[56] A. Gleadall, J. Pan, M.-A. Kruft, M. Kellomäki, *Acta Biomater.* **2014**, *10*, 2223.
[57] P. Gentile, V. Chiono, I. Carmagnola, P. Hatton, *Int. J. Mol. Sci.* **2014**, *15*, 3640.
[58] S. H. Park, D. S. Park, J. W. Shin, Y. G. Kang, H. K. Kim, T. R. Yoon, J.-W. Shin, *J. Mater. Sci. Mater. Med.* **2012**, *23*, 2671.
[59] A. Prasad, B. Kandasubramanian, *Polym. Technol. Mater.* **2019**, *58*, 1365.
[60] D. W. Hutmacher, T. Schantz, I. Zein, K. W. Ng, S. H. Teoh, K. C. Tan, *J. Biomed. Mater. Res.* **2001**, *55*, 203.
[61] J. Korpela, A. Kokkari, H. Korhonen, M. Malin, T. Narhi, J. Seppalea, *J. Biomed. Mater. Res., Part B* **2013**, *101*, 610.
[62] F. Wang, L. Shor, A. Darling, S. Khalil, W. Sun, S. Güçeri, A. Lau, *Rapid Prototyping J.* **2004**, *10*, 42.
[63] D. Muller, H. Chim, A. Bader, M. Whiteman, J.-T. Schantz, *Stem Cells Int* **2011**, *2011*, 547247.
[64] Y.-Q. Zhao, J.-H. Yang, X. Ding, X. Ding, S. Duan, F.-J. Xu, *Bioact. Mater.* **2020**, *5*, 185.
[65] G. Ciardelli, V. Chiono, G. Vozzi, M. Pracella, A. Ahluwalia, N. Barbani, C. Cristallini, P. Giusti, *Biomacromolecules* **2005**, *6*, 1961.
[66] H.-W. Kang, S. J. Lee, I. K. Ko, C. Kengla, J. J. Yoo, A. Atala, *Nat. Biotechnol.* **2016**, *34*, 312.
[67] S. M. S. Gruber, P. Ghosh, K. W. Mueller, P. W. Whitlock, C. Y. Lin, *J. Vis. Exp.* **2019**, *2019*, 2.
[68] J. M. Sobral, S. G. Caridade, R. A. Sousa, J. F. Mano, R. L. Reis, *Acta Biomater.* **2011**, *7*, 1009.

[69] H. Seyednejad, D. Gawlitta, W. J. A. Dhert, C. F. Van Nostrum, T. Vermonden, W. E. Hennink, *Acta Biomater.* **2011**, *7*, 1999.
[70] H. Wang, C. A. Van Blitterswijk, *Biomaterials* **2010**, *31*, 4322.
[71] H. A. Declercq, T. Desmet, E. E. M. Berneel, P. Dubruel, M. J. Cornelissen, *Acta Biomater.* **2013**, *9*, 7699.
[72] P. Yilgor, G. Yilmaz, M. B. Onal, I. Solmaz, S. Gundogdu, S. Keskil, R. A. Sousa, R. L. Reis, N. Hasirci, V. Hasirci, *J. Tissue Eng. Regener. Med.* **2013**, *7*, 687.
[73] M. Chen, D. Q. S. Le, A. Baatrup, J. V. Nygaard, S. Hein, L. Bjerre, M. Kassem, X. Zou, C. Bünger, *Acta Biomater.* **2011**, *7*, 2244.
[74] J. Li, M. Chen, X. Wei, Y. Hao, J. Wang, *Materials* **2017**, *10*, 831.
[75] S. N. Parikh, *J. Postgrad. Med.* **2002**, *48*, 142.
[76] J. P. Temple, D. L. Hutton, B. P. Hung, P. Y. Huri, C. A. Cook, R. Kondragunta, X. Jia, W. L. Grayson, *J. Biomed. Mater. Res., Part A* **2014**, *102*, 4317.
[77] D. L. Hutton, E. M. Moore, J. M. Gimble, W. L. Grayson, *Tissue Eng., Part A* **2013**, *19*, 2076.
[78] R. Trombetta, J. A. Inzana, E. M. Schwarz, S. L. Kates, H. A. Awad, *Ann. Biomed. Eng.* **2017**, *45*, 23.
[79] E. Nyberg, A. Rindone, A. Dorafshar, W. L. Grayson, *Tissue Eng., Part A* **2017**, *23*, 503.
[80] A. Bruyas, F. Lou, A. M. Stahl, M. Gardner, W. Maloney, S. Goodman, Y. P. Yang, *J. Mater. Res.* **2018**, *33*, 1948.
[81] N. Thuaksuban, R. Pannak, P. Boonyaphiphat, N. Monmaturapoj, *Biomed. Mater. Eng.* **2018**, *29*, 253.
[82] C. X. F. Lam, D. W. Hutmacher, J.-T. Schantz, M. A. Woodruff, S. H. Teoh, *J. Biomed. Mater. Res., Part A* **2009**, *90A*, 906.
[83] A. Khojasteh, H. Behnia, F. S. Hosseini, M. M. Dehghan, P. Abbasnia, F. M. Abbas, *J. Biomed. Mater. Res., Part B* **2013**, *101 B*, 848.
[84] A. Polini, D. Pisignano, M. Parodi, R. Quarto, S. Scaglione, *PLoS One* **2011**, *6*, 26211.
[85] N. Xu, X. Ye, D. Wei, J. Zhong, Y. Chen, G. Xu, D. He, *ACS Appl. Mater. Interfaces* **2014**, *6*, 14952.
[86] M. E. Alemán-Domínguez, E. Giusto, Z. Ortega, M. Tamaddon, A. N. Benítez, C. Liu, *J. Biomed. Mater. Res., Part B* **2019**, *107*, 521.
[87] J. B. Lee, J. E. Kim, M. S. Bae, S. A. Park, D. A. Balikov, H. J. Sung, H. B. Jeon, H. K. Park, S. H. Um, K. S. Lee, I. K. Kwon, *Polymers* **2016**, *8*, 49.
[88] L. L. Hench, J. R. Jones, *Front. Bioeng. Biotechnol.* **2015**, *3*, 194.
[89] P. S. P. Poh, D. W. Hutmacher, M. M. Stevens, M. A. Woodruff, *Biofabrication* **2013**, *5*, 045005.
[90] P. S. P. Poh, D. W. Hutmacher, B. M. Holzapfel, A. K. Solanki, M. M. Stevens, M. A. Woodruff, *Acta Biomater.* **2016**, *30*, 319.
[91] C. Wang, C. Meng, Z. Zhang, Q. Zhu, *Ceram. Int.* **2022**, *48*, 7491.
[92] B. P. Hung, B. A. Naved, E. L. Nyberg, M. Dias, C. A. Holmes, J. H. Elisseeff, A. H. Dorafshar, W. L. Grayson, *ACS Biomater. Sci. Eng.* **2016**, *2*, 1806.
[93] J. C. Silva, M. S. Carvalho, R. N. Udangawa, C. S. Moura, J. M. S. Cabral, C. L. Da Silva, F. C. Ferreira, D. Vashishth, R. J. Linhardt, *J. Biomed. Mater. Res., Part B* **2020**, *108*, 2153.
[94] S. J. Lee, D. Lee, T. R. Yoon, H. K. Kim, H. H. Jo, J. S. Park, J. H. Lee, W. D. Kim, I. K. Kwon, S. A. Park, *Acta Biomater.* **2016**, *40*, 182.
[95] S. A. Park, J. B. Lee, Y. E. Kim, J. E. Kim, J. H. Lee, J.-W. Shin, I. K. Kwon, W. Kim, *Macromol. Res.* **2014**, *22*, 882.
[96] J. S. Park, S. J. Lee, H. H. Jo, J. H. Lee, W. D. Kim, J. Y. Lee, S. A. Park, *J. Ind. Eng. Chem.* **2017**, *46*, 175.
[97] P. F. Costa, C. Vaquette, Q. Zhang, R. L. Reis, S. Ivanovski, D. W. Hutmacher, *J. Clin. Periodontol.* **2014**, *41*, 283.
[98] C. H. Lee, J. Hajibandeh, T. Suzuki, A. Fan, P. Shang, J. J. Mao, *Tissue Eng., Part A* **2014**, *20*, 1342.
[99] Y. Bai, Y. Bai, K. Matsuzaka, S. Hashimoto, T. Fukuyama, L. Wu, T. Miwa, X. Liu, X. Wang, T. Inoue, *Bone* **2011**, *48*, 1417.
[100] K. Kim, C. H. Lee, B. K. Kim, J. J. Mao, *J. Dent. Res.* **2010**, *89*, 842.
[101] C. Vaquette, W. Fan, Y. Xiao, S. Hamlet, D. W. Hutmacher, S. Ivanovski, *Biomaterials* **2012**, *33*, 5560.
[102] S. Soliman, S. Pagliari, A. Rinaldi, G. Forte, R. Fiaccavento, F. Pagliari, O. Franzese, M. Minieri, P. Di Nardo, S. Licoccia, *Acta Biomater.* **2010**, *6*, 1227.
[103] A. Szojka, K. Lalh, S. H. J. Andrews, N. M. Jomha, M. Osswald, A. B. Adesida, *Bioprinting* **2017**, *8*, 1.
[104] P. Zheng, X. Hu, Y. Lou, K. Tang, *Med. Sci. Monit.* **2019**, *25*, 7361.
[105] S. J. Wang, Z. Z. Zhang, D. Jiang, Y. S. Qi, H. J. Wang, J. Y. Zhang, J. X. Ding, J. K. Yu, *Polymers* **2016**, *8*, 200.
[106] Y.-H. Hsieh, B.-Y. Shen, Y.-H. Wang, B. Lin, H.-M. Lee, M.-F. Hsieh, *Int. J. Mol. Sci.* **2018**, *19*, 1125.
[107] S. Van Uden, J. Silva-Correia, V. M. Correlo, J. M. Oliveira, R. L. Reis, *Biofabrication* **2015**, *7*, 015008.
[108] D. O. Visscher, E. J. Bos, M. Peeters, N. V. Kuzmin, M. L. Groot, M. N. Helder, P. P. M. Van Zuijlen, *Tissue Eng., Part C* **2016**, *22*, 573.
[109] D. S. Chan, N. Fnais, I. Ibrahim, S. J. Daniel, J. Manoukian, *Int. J. Pediatr. Otorhinolaryngol.* **2019**, *123*, 38.
[110] S. Y. Jung, S. J. Lee, H. Y. Kim, H. S. Park, Z. Wang, H. J. Kim, J. J. Yoo, S. M. Chung, H. S. Kim, *Biofabrication* **2016**, *8*, 045015.
[111] A. A. Mäkitie, J. Korpela, L. Elomaa, M. Reivonen, A. Kokkari, M. Malin, H. Korhonen, X. Wang, J. Salo, E. Sihvo, M. Salmi, J. Partanen, K.-S. Paloheimo, J. Tuomi, T. Närhi, J. Seppälä, *Acta Otolaryngol.* **2013**, *133*, 412.
[112] D. Y. Lee, S. A. Park, S. J. Lee, T. H. Kim, S. H. Oh, J. H. Lee, S. K. Kwon, *Laryngoscope* **2016**, *126*, E304.
[113] H. S. Park, H. J. Park, J. Lee, P. Kim, J. S. Lee, Y. J. Lee, Y. B. Seo, D. Y. Kim, O. Ajiteru, O. J. Lee, C. H. Park, *Tissue Eng. Regener. Med.* **2018**, *15*, 415.
[114] K. J. Tsai, S. Dixon, L. R. Hale, A. Darbyshire, D. Martin, A. de Mel, *npj Regener. Med.* **2017**, *2*, 1.
[115] M. Centola, A. Rainer, C. Spadaccio, S. De Porcellinis, J. A. Genovese, M. Trombetta, *Biofabrication* **2010**, *2*, 014102.
[116] B. Rai, S. H. Teoh, D. W. Hutmacher, T. Cao, K. H. Ho, *Biomaterials* **2005**, *26*, 3739.
[117] J. Holländer, N. Genina, H. Jukarainen, M. Khajeheian, A. Rosling, E. Mäkilä, N. Sandler, *J. Pharm. Sci.* **2016**, *105*, 2665.
[118] E. Y. Teo, S.-Y. Ong, M. S. Khoon Chong, Z. Zhang, J. Lu, S. Moochhala, B. Ho, S.-H. Teoh, *Biomaterials* **2011**, *32*, 279.
[119] D. H. Ballard, U. Jammalamadaka, K. Tappa, J. A. Weisman, C. J. Boyer, J. S. Alexander, P. K. Woodard, *3D Print. Med.* **2018**, *4*, 13.
[120] P. Gunatillake, *Eur. Cells Mater.* **2003**, *5*, 1.
[121] K. Miller, J. E. Hsu, L. J. Soslowsky, *Comprehensive Biomaterials*, Elsevier, Netherlands **2011**, pp. 257–279.
[122] M. Shunmugasundaram, A. A. B. Maughal, M. Ajay Kumar, *Mater. Today Proc.* **2020**, *27*, 1596.
[123] A. J. R. Lasprilla, G. A. R. Martinez, B. H. Lunelli, A. L. Jardini, R. M. Filho, *Biotechnol. Adv.* **2012**, *30*, 321.
[124] R. A. Auras, L.-T. Lim, S. E. M. Selke, H. Tsuji, *Poly(Lactic Acid): Synthesis, Structures, Properties, Processing, and Applications*, Wiley, Hoboken **2010**.
[125] S. Farah, D. G. Anderson, R. Langer, *Adv. Drug Delivery Rev.* **2016**, *107*, 367.
[126] A. Abdulkhani, J. Hosseinzadeh, A. Ashori, S. Dadashi, Z. Takzare, *Polym. Test.* **2014**, *35*, 73.
[127] J. Ambrosio-Martín, M. J. Fabra, A. Lopez-Rubio, J. M. Lagaron, *Cellulose* **2015**, *22*, 1201.
[128] R. M. Rasal, A. V. Janorkar, D. E. Hirt, *Prog. Polym. Sci.* **2010**, *35*, 338.
[129] A. V. Janorkar, A. T. Metters, D. E. Hirt, *Macromolecules* **2004**, *37*, 9151.
[130] S. Liu, G. Wu, X. Zhang, J. Yu, M. Liu, Y. Zhang, P. Wang, X. Yin, J. Zhang, F. Li, M. Zhang, *J. Text. Inst.* **2019**, *110*, 1596.
[131] B. Tyler, D. Gullotti, A. Mangraviti, T. Utsuki, H. Brem, *Adv. Drug Delivery Rev.* **2016**, *107*, 163.

[132] T. M. Rankin, N. A. Giovinco, D. J. Cucher, G. Watts, B. Hurwitz, D. G. Armstrong, *J. Surg. Res.* **2014**, *189*, 193.
[133] L. Raddatz, M. Kirsch, D. Geier, J. Schaeske, K. Acreman, R. Gentsch, S. Jones, A. Karau, T. Washington, M. Stiesch, T. Becker, S. Beutel, T. Scheper, A. Lavrentieva, *J. Biomater. Appl.* **2018**, *33*, 281.
[134] V. DeStefano, S. Khan, A. Tabada, *Eng. Regener.* **2020**, *1*, 76.
[135] J. Jóźwicka, K. Gzyra-Jagieła, A. Gutowska, K. Twarowska-Schmidt, M. Ciepliński, *Fibres Text. East. Eur.* **2012**, *96*, 135.
[136] J. K. Placone, A. J. Engler, *Adv. Healthcare Mater.* **2018**, *7*, 1701161.
[137] M. C. Wurm, T. Möst, B. Bergauer, D. Rietzel, F. W. Neukam, S. C. Cifuentes, C. V. Wilmowsky, *J. Biol. Eng.* **2017**, *11*, 29.
[138] G. Cicala, D. Giordano, C. Tosto, G. Filippone, A. Recca, I. Blanco, *Materials* **2018**, *11*, 1191.
[139] C. Wang, L. M. Smith, W. Zhang, M. Li, G. Wang, S. Q. Shi, H. Cheng, S. Zhang, *Polymers* **2019**, *11*, 1146.
[140] K. A. Evans, Z. C. Kennedy, B. W. Arey, J. F. Christ, H. T. Schaef, S. K. Nune, R. L. Erikson, *ACS Appl. Mater. Interfaces* **2018**, *10*, 15112.
[141] J. S. Chohan, R. Singh, *Rapid Prototyp. J.* **2017**, *23*, 495.
[142] M. K. Kim, I. H. Lee, H.-C. Kim, *Int. J. Precis. Eng. Manuf.* **2018**, *19*, 137.
[143] A. Valerga, M. Batista, S. Fernandez-Vidal, A. Gamez, *Polymers* **2019**, *11*, 566.
[144] K.-C. Feng, A. Pinkas-Sarafova, V. Ricotta, M. Cuiffo, L. Zhang, Y. Guo, C.-C. Chang, G. P. Halada, M. Simon, M. Rafailovich, *Soft Matter* **2018**, *14*, 9838.
[145] V. Guduric, C. Metz, R. Siadous, R. Bareille, R. Levato, E. Engel, J.-C. Fricain, R. Devillard, O. Luzanin, S. Catros, *J. Mater. Sci. Mater. Med.* **2017**, *28*, 1.
[146] C.-H. Cheng, Y.-W. Chen, A. Kai-Xing Lee, C.-H. Yao, M.-Y. Shie, *J. Mater. Sci. Mater. Med.* **2019**, *30*, 78.
[147] J.-H. Shim, T.-S. Moon, M.-J. Yun, Y.-C. Jeon, C.-M. Jeong, D.-W. Cho, J.-B. Huh, *J. Mater. Sci. Mater. Med.* **2012**, *23*, 2993.
[148] A. Grémare, V. Guduric, R. Bareille, V. Heroguez, S. Latour, N. L'heureux, J.-C. Fricain, S. Catros, D. Le Nihouannen, *J. Biomed. Mater. Res., Part A* **2018**, *106*, 887.
[149] L. R. Jaidev, K. Chatterjee, *Mater. Des.* **2019**, *161*, 44.
[150] X. Chen, C. Gao, J. Jiang, Y. Wu, P. Zhu, G. Chen, *Biomed. Mater.* **2019**, *14*, 065003.
[151] S. Adriana Martel Estrada, I. Olivas Armendáriz, A. Torres García, J. Francisco Hernández Paz, C. Alejandra Rodríguez González, *Int. J. Compos. Mater.* **2017**, *7*, 144.
[152] T. Distler, N. Fournier, A. Grünewald, C. Polley, H. Seitz, R. Detsch, A. R. Boccaccini, *Front. Bioeng. Biotechnol.* **2020**, *8*, 552.
[153] T. Serra, J. A. Planell, M. Navarro, *Acta Biomater.* **2013**, *9*, 5521.
[154] J. Russias, E. Saiz, S. Deville, K. Gryn, G. Liu, R. K. Nalla, A. P. Tomsia, *J. Biomed. Mater. Res., Part A* **2007**, *83A*, 434.
[155] C. Murphy, K. C. R. Kolan, M. Long, W. Li, M. C. Leu, J. A. Semon, D. E. Day, Proceedings of the 27th Annual International Solid Freeform Fabrication Symposium, University of Texas, Austin **2016**, p. 1718.
[156] D. Wu, A. Spanou, A. Diez-Escudero, C. Persson, *J. Mech. Behav. Biomed. Mater.* **2020**, *103*, 103608.
[157] Z. Wu, J. Zhao, W. Wu, P. Wang, B. Wang, G. Li, S. Zhang, *Materials* **2018**, *11*, 1357.
[158] N. Sears, P. Dhavalikar, M. Whitely, E. Cosgriff-Hernandez, *Biofabrication* **2017**, *9*, 025020.
[159] A. Goyanes, A. B. M. Buanz, A. W. Basit, S. Gaisford, *Int. J. Pharm.* **2014**, *476*, 88.
[160] J. J. Water, A. Bohr, J. Boetker, J. Aho, N. Sandler, H. M. Nielsen, J. Rantanen, *J. Pharm. Sci.* **2015**, *104*, 1099.
[161] J. Boetker, J. J. Water, J. Aho, L. Arnfast, A. Bohr, J. Rantanen, *Eur. J. Pharm. Sci.* **2016**, *90*, 47.
[162] J. Skowyra, K. Pietrzak, M. A. Alhnan, *Eur. J. Pharm. Sci.* **2015**, *68*, 11.
[163] A. Goyanes, J. Wang, A. Buanz, R. Martínez-Pacheco, R. Telford, S. Gaisford, A. W. Basit, *Mol. Pharm.* **2015**, *12*, 4077.
[164] M. Saviano, R. P. Aquino, P. Del Gaudio, F. Sansone, P. Russo, *Int. J. Pharm.* **2019**, *561*, 1.
[165] T. Tagami, N. Nagata, N. Hayashi, E. Ogawa, K. Fukushige, N. Sakai, T. Ozeki, *Int. J. Pharm.* **2018**, *543*, 361.
[166] X. Xu, J. Zhao, M. Wang, L. Wang, J. Yang, *Sci. Rep.* **2019**, *9*, 1.
[167] J. A. Weisman, D. H. Ballard, U. Jammalamadaka, K. Tappa, J. Sumerel, H. B. D'agostino, D. K. Mills, P. K. Woodard, *Acad. Radiol.* **2019**, *26*, 270.
[168] M. A. Luzuriaga, D. R. Berry, J. C. Reagan, R. A. Smaldone, J. J. Gassensmith, *Lab Chip* **2018**, *18*, 1223.
[169] X. Farto-Vaamonde, G. Auriemma, R. P. Aquino, A. Concheiro, C. Alvarez-Lorenzo, *Eur. J. Pharm. Biopharm.* **2019**, *141*, 100.
[170] K. Deng, H. Chen, Y. Zhao, Y. Zhou, Y. Wang, Y. Sun, *PLoS One* **2018**, *13*, e0201777.
[171] H. Tamai, K. Igaki, E. Kyo, K. Kosuga, A. Kawashima, S. Matsui, H. Komori, T. Tsuji, S. Motohara, H. Uehata, *Circulation* **2000**, *102*, 399.
[172] C. Agrawal, K. Haas, D. Leopold, H. Clark, *Biomaterials* **1992**, *13*, 176.
[173] W. H. Kaesemeyer, K. G. Sprankle, J. N. Kremsky, W. Lau, M. N. Helmus, G. S. Ghatnekar, *Coron. Artery Dis.* **2013**, *24*, 516.
[174] S. A. Park, S. J. Lee, K. S. Lim, I. H. Bae, J. H. Lee, W. D. Kim, M. H. Jeong, J.-K. Park, *Mater. Lett.* **2015**, *141*, 355.
[175] D. S. Sim, M. H. Jeong, *Chonnam Med. J.* **2017**, *53*, 187.
[176] C. W. Foster, M. P. Down, Y. Zhang, X. Ji, S. J. Rowley-Neale, G. C. Smith, P. J. Kelly, C. E. Banks, *Sci. Rep.* **2017**, *7*, 1.
[177] M. D. Symes, P. J. Kitson, J. Yan, C. J. Richmond, G. J. T. Cooper, R. W. Bowman, T. Vilbrandt, L. Cronin, *Nat. Chem.* **2012**, *4*, 349.
[178] K. Scida, P. W. Stege, G. Haby, G. A. Messina, C. D. García, *Anal. Chim. Acta* **2011**, *691*, 6.
[179] L. L. Zhang, X. S. Zhao, *Chem. Soc. Rev.* **2009**, *38*, 2520.
[180] C. L. Manzanares-Palenzuela, F. Novotný, P. Krupička, Z. Sofer, M. Pumera, *Anal. Chem.* **2018**, *90*, 5753.
[181] E. M. Richter, D. P. Rocha, R. M. Cardoso, E. M. Keefe, C. W. Foster, R. A. A. Munoz, C. E. Banks, *Anal. Chem.* **2019**, *91*, 12844.
[182] C. L. Manzanares-Palenzuela, S. Hermanova, Z. Sofer, M. Pumera, *Nanoscale* **2019**, *11*, 12124.
[183] S. Krachunov, A. Casson, *Sensors* **2016**, *16*, 1635.
[184] K. A. Singh Gurpreet, K. Tanurajvir, K. Ravinder, *Int. J. Pharmacol. Pharm. Sci.* **2014**, *1*, 30.
[185] N. Régibeau, J. Hurlet, R. G. Tilkin, F. Lombart, B. Heinrichs, C. Grandfils, *Mater. Today Commun.* **2020**, *24*, 101208.
[186] T. Feuerbach, S. Callau-Mendoza, M. Thommes, *Pharm. Dev. Technol.* **2019**, *24*, 487.
[187] F. Danhier, E. Ansorena, J. M. Silva, R. Coco, A. Le Breton, V. Préat, *J. Controlled Release* **2012**, *161*, 505.
[188] S. Sharma, A. Parmar, S. Kori, R. Sandhir, *TrAC, Trends Anal. Chem.* **2016**, *80*, 30.
[189] W. Zhao, J. Li, K. Jin, W. Liu, X. Qiu, C. Li, *Mater. Sci. Eng. C* **2016**, *59*, 1181.
[190] H. Zhou, J. G. Lawrence, S. B. Bhaduri, *Acta Biomater.* **2012**, *8*, 1999.
[191] J. Yu, A.-R. Lee, W.-H. Lin, C.-W. Lin, Y.-K. Wu, W.-B. Tsai, *Tissue Eng., Part A* **2014**, *20*, 1896.
[192] X. Sun, C. Xu, G. Wu, Q. Ye, C. Wang, *Polymers* **2017**, *9*, 189.
[193] H. K. Makadia, S. J. Siegel, *Polymers* **2011**, *3*, 1377.
[194] H.-J. Yen, C.-S. Tseng, S.-H. Hsu, C.-L. Tsai, *Biomed. Microdevices* **2009**, *11*, 615.
[195] H.-J. Sung, C. Meredith, C. Johnson, Z. S. Galis, *Biomaterials* **2004**, *25*, 5735.
[196] J. Kim, S. Mcbride, B. Tellis, P. Alvarez-Urena, Y.-H. Song, D. D. Dean, V. L. Sylvia, H. Elgendy, J. Ong, J. O. Hollinger, *Biofabrication* **2012**, *4*, 025003.
[197] E. Carlier, S. Marquette, C. Peerboom, K. Amighi, J. Goole, *Int. J. Pharm.* **2021**, *597*, 120337.

[198] E. Akaraonye, T. Keshavarz, I. Roy, *J. Chem. Technol. Biotechnol.* **2010**, *85*, 732.
[199] T. Keshavarz, I. Roy, *Curr. Opin. Microbiol.* **2010**, *13*, 321.
[200] A. Shrivastav, H.-Y. Kim, Y.-R. Kim, *Biomed. Res. Int.* **2013**, *2013*, 581684.
[201] S. Pachiyappan, D. Shanmuganatham Selvanantham, S. S. Kuppa, S. Chandrasekaran, A. V. Samrot, *IET Nanobiotechnol.* **2019**, *13*, 416.
[202] Z. A. Raza, S. Abid, I. M. Banat, *Int. Biodeterior. Biodegrad.* **2018**, *126*, 45.
[203] D. Puppi, G. Pecorini, F. Chiellini, *Bioengineering* **2019**, *6*, 108.
[204] C.-S. Wu, H.-T. Liao, *J. Polym. Eng.* **2017**, *37*, 689.
[205] C. S. Wu, H. T. Liao, *Express Polym. Lett.* **2017**, *11*, 187.
[206] C.-S. Wu, H.-T. Liao, Y.-X. Cai, *Polym. Degrad. Stab.* **2017**, *140*, 55.
[207] F. Valentini, A. Dorigato, D. Rigotti, A. Pegoretti, *J. Polym. Environ.* **2019**, *27*, 1333.
[208] X. Ye, L. Li, Z. Lin, W. Yang, M. Duan, L. Chen, Y. Xia, Z. Chen, Y. Lu, Y. Zhang, *Carbohydr. Polym.* **2018**, *202*, 106.
[209] B. Aráoz, E. Karakaya, A. González Wusener, R. Detsch, J. Bizzotto, G. Gueron, A. R. Boccaccini, É. B. Hermida, *J. Mater. Res.* **2021**, *36*, 4000.
[210] A. Haryńska, J. Kucinska-Lipka, A. Sulowska, I. Gubanska, M. Kostrzewa, H. Janik, *Materials* **2019**, *12*, 887.
[211] G. A. Skarja, K. A. Woodhouse, *J. Appl. Polym. Sci.* **2000**, *75*, 1522.
[212] J.-Y. Zhang, B. A. Doll, E. J. Beckman, J. O. Hollinger, *Tissue Eng.* **2003**, *9*, 1143.
[213] S. A. Guelcher, K. M. Gallagher, J. E. Didier, D. B. Klinedinst, J. S. Doctor, A. S. Goldstein, G. L. Wilkes, E. J. Beckman, J. O. Hollinger, *Acta Biomater.* **2005**, *1*, 471.
[214] S. A. Guelcher, *Tissue Eng., Part B* **2008**, *14*, 3.
[215] J. Kucińska-Lipka, I. Gubanska, M. Pokrywczynska, H. Ciesliński, N. Filipowicz, T. Drewa, H. Janik, *Polym. Bull.* **2018**, *75*, 1957.
[216] J. Kucinska-Lipka, I. Gubanska, M. Strankowski, H. Cieśliński, N. Filipowicz, H. Janik, *Mater. Sci. Eng., C* **2017**, *75*, 671.
[217] M. Boffito, S. Sartori, G. Ciardelli, *Polym. Int.* **2014**, *63*, 2.
[218] V. Chiono, S. Sartori, A. Rechichi, C. Tonda-Turo, G. Vozzi, F. Vozzi, M. D'acunto, C. Salvadori, F. Dini, G. Barsotti, F. Carlucci, S. Burchielli, S. Nicolino, C. Audisio, I. Perroteau, P. Giusti, G. Ciardelli, *Macromol. Biosci.* **2011**, *11*, 245.
[219] A. Silvestri, S. Sartori, M. Boffito, C. Mattu, A. M. Di Rienzo, F. Boccafoschi, G. Ciardelli, F. Boccafoschi, G. Ciardelli, *J. Biomed. Mater. Res., Part B* **2014**, *102*, 1002.
[220] A. Kiziltay, A. Marcos-Fernandez, J. San Roman, R. A. Sousa, R. L. Reis, V. Hasirci, N. Hasirci, *J. Tissue Eng. Regener. Med.* **2015**, *9*, 930.
[221] A. Haryńska, I. Gubanska, J. Kucinska-Lipka, H. Janik, *Polymers* **2018**, *10*, 1304.
[222] N. J. Lores, X. Hung, M. H. Talou, G. A. Abraham, P. C. Caracciolo, *Polym. Adv. Technol.* **2021**, *32*, 3309.
[223] S. Camarero-Espinosa, A. Calore, A. Wilbers, J. Harings, L. Moroni, *Acta Biomater.* **2020**, *102*, 192.
[224] S. Camarero-Espinosa, C. Tomasina, A. Calore, L. Moroni, *Mater. Today Bio* **2020**, *6*, 100051.
[225] V. Chiono, P. Mozetic, M. Boffito, S. Sartori, E. Gioffredi, A. Silvestri, A. Rainer, S. M. Giannitelli, M. Trombetta, D. Nurzynska, F. Di Meglio, C. Castaldo, R. Miraglia, S. Montagnani, G. Ciardelli, *Interfaces Focus* **2014**, *4*, 20130045.
[226] M. Boffito, F. Di Meglio, P. Mozetic, S. M. Giannitelli, I. Carmagnola, C. Castaldo, D. Nurzynska, A. M. Sacco, R. Miraglia, S. Montagnani, N. Vitale, M. Brancaccio, G. Tarone, F. Basoli, A. Rainer, M. Trombetta, G. Ciardelli, V. Chiono, *PLoS One* **2018**, *13*, 0199896.
[227] A. Güney, C. Gardiner, A. Mccormack, J. Malda, D. Grijpma, *Bioengineering* **2018**, *5*, 99.
[228] M. Chung, N. Radacsi, C. Robert, E. D. McCarthy, A. Callanan, N. Conlisk, P. R. Hoskins, V. Koutsos, *3D Print. Med.* **2018**, *4*, 2.
[229] R. Faletti, M. Gatti, A. Cosentino, L. Bergamasco, E. Cura Stura, D. Garabello, G. Pennisi, S. Salizzoni, S. Veglia, D. Ottavio, M. Rinaldi, P. Fonio, *J. Cardiovasc. Comput. Tomogr.* **2018**, *12*, 391.
[230] R. Natividad, M. Del Rosario, P. C. Y. Chen, C.-H. Yeow, *Soft Rob.* **2018**, *5*, 304.
[231] J. Domínguez-Robles, C. Mancinelli, E. Mancuso, I. García-Romero, B. F. Gilmore, L. Casettari, E. Larrañeta, D. A. Lamprou, *Pharmaceutics* **2020**, *12*, 63.
[232] A. Haryńska, I. Carayon, P. Kosmela, A. Brillowska-Dąbrowska, M. Łapiński, J. Kucińska-Lipka, H. Janik, *Materials* **2020**, *13*, 4457.
[233] D. Bandelli, J. Alex, C. Weber, U. S. Schubert, *Macromol. Rapid Commun.* **2020**, *41*, 1900560.
[234] J. Urquijo, G. Guerrica-Echevarría, J. I. Eguiazábal, *J. Appl. Polym. Sci.* **2015**, *132*.
[235] A. K. Matta, R. U. Rao, K. N. S. Suman, V. Rambabu, *Procedia Mater. Sci.* **2014**, *6*, 1266.
[236] J. Fu, H. Yin, X. Yu, C. Xie, H. Jiang, Y. Jin, F. Sheng, *Int. J. Pharm.* **2018**, *549*, 370.
[237] L. D. Albrecht, S. W. Sawyer, P. Soman, *3D Print. Addit. Manuf.* **2016**, *3*, 106.
[238] H. Liu, H. He, B. Huang, *Macromol. Mater. Eng.* **2020**, *305*, 2000295.
[239] A. Guerra, P. Cano, M. Rabionet, T. Puig, J. Ciurana, *Materials* **2018**, *11*, 1679.
[240] R. Guo, Z. Ren, X. Jia, H. Bi, H. Yang, T. Ji, M. Xu, L. Cai, *Polymers* **2019**, *11*, 1589.
[241] R. Guo, Z. Ren, H. Bi, M. Xu, L. Cai, *Polymers* **2019**, *11*, 549.
[242] S. Wang, K. De Clerck, L. Cardon, Int. Conf. Polymers and Moulds Innovations - PMI 2018, Institute of Polymers and Composites, University of Minho, Portugal, **2018**.
[243] J. V. Ecker, I. Burzic, A. Haider, S. Hild, H. Rennhofer, *Polym. Test.* **2019**, *78*, 105929.
[244] S. Guessasma, S. Belhabib, H. Nouri, *Rapid Prototyping J.* **2020**, *26*, 122.
[245] L. M. W. K. Gunaratne, R. A. Shanks, *Polym. Eng. Sci.* **2008**, *48*, 1683.
[246] M. A. Abdelwahab, A. Flynn, B.-S. Chiou, S. Imam, W. Orts, E. Chiellini, *Polym. Degrad. Stab.* **2012**, *97*, 1822.
[247] S. Wang, K. De Clerck, L. Cardon, Int. Conf. Polym. Mould. Innov. **2018**.
[248] J. V. Ecker, I. Burzic, A. Haider, S. Hild, H. Rennhofer, *Polym. Test.* **2019**, *78*, 105929.
[249] P. Menčík, R. Přikryl, I. Stehnová, V. Melčová, S. Kontárová, S. Figalla, P. Alexy, J. Bočkaj, *Materials* **2018**, *11*, 1893.
[250] B. Kaygusuz, S. Özerinç, *J. Appl. Polym. Sci.* **2019**, *136*, 48154.
[251] J. Gonzalez Ausejo, J. Rydz, M. Musioł, W. Sikorska, M. Sobota, J. Włodarczyk, G.ż Adamus, H. Janeczek, I. Kwiecień, A. Hercog, B. Johnston, H. R. Khan, V. Kannappan, K. R. Jones, M. R. Morris, G. Jiang, I. Radecka, M. Kowalczuk, *Polym. Degrad. Stab.* **2018**, *152*, 191.
[252] W. Kosorn, M. Sakulsumbat, P. Uppanan, P. Kaewkong, S. Chantaweroad, J. Jitsaard, K. Sitthiseripratip, W. Janvikul, *J. Biomed. Mater. Res., Part B* **2017**, *105*, 1141.
[253] W. Kosorn, P. Wutticharoenmongkol, *Int. J. Polym. Sci.* **2021**, *2021*, 6689789.
[254] J. Idaszek, A. Bruinink, W. więszkowski, *J. Biomed. Mater. Res., Part A* **2015**, *103*, 2394.
[255] J. M. Hong, B. J. Kim, J.-H. Shim, K. S. Kang, K.-J. Kim, J. W. Rhie, H. J. Cha, D.-W. Cho, *Acta Biomater.* **2012**, *8*, 2578.
[256] T.-H. Kim, Y.-P. Yun, Y.-E. Park, S.-H. Lee, W. Yong, J. Kundu, J. W. Jung, J.-H. Shim, D.-W. Cho, S. E. Kim, H.-R. Song, *Biomed. Mater.* **2014**, *9*, 025008.
[257] R. Dixit, U. A. Boelsterli, *Drug Discovery Today* **2007**, *12*, 336.

[258] F. Zavřel, M. Novák, J. Kroupová, C. Beveridge, F. Štěpánek, G. Ruphuy, *Adv. Eng. Mater.* **2021**, 2100820.
[259] Y. S. Cho, S. Choi, S.-H. Lee, K. K. Kim, Y.-S. Cho, *Eur. Polym. J.* **2019**, *113*, 340.
[260] M. Jafari, Z. Paknejad, M. R. Rad, S. R. Motamedian, M. J. Eghbal, N. Nadjmi, A. Khojasteh, N. Nadjmi, A. Khojasteh, *J. Biomed. Mater. Res., Part B* **2017**, *105*, 431.
[261] F. Liang, H. Leland, B. Jedrzejewski, A. Auslander, S. Maniskas, J. Swanson, M. Urata, J. Hammoudeh, W. Magee, *J. Craniofac. Surg.* **2018**, *29*, 584.
[262] P. Korn, T. Ahlfeld, F. Lahmeyer, D. Kilian, P. Sembdner, R. Stelzer, W. Pradel, A. Franke, M. Rauner, U. Range, B. Stadlinger, A. Lode, G. Lauer, M. Gelinsky, *Front. Bioeng. Biotechnol.* **2020**, *8*, 217.
[263] G. Ahn, J.-S. Lee, W.-S. Yun, J.-H. Shim, U.-L. Lee, *J. Craniofac. Surg.* **2018**, *29*, 1880.
[264] P. Tack, J. Victor, P. Gemmel, L. Annemans, *Biomed. Eng. Online* **2016**, *15*, 1.
[265] M. A. Mirza, Z. Iqbal, *Curr. Pharm. Des.* **2019**, *24*, 5081.
[266] M. H. Eng, D. D. Wang, A. B. Greenbaum, N. Gheewala, D. Kupsky, T. Aka, T. Song, B. J. Kendall, J. Wyman, E. Myers, M. Forbes, W. W. O'neill, *Catheter. Cardiovasc. Interv.* **2018**, *92*, 401.
[267] Z. Wang, Y. Liu, H. Luo, C. Gao, J. Zhang, Y. Dai, *Acta Cardiol. Sin.* **2017**, *33*, 664.
[268] M. H. Ali, S. Batai, D. Sarbassov, *Rapid Prototyp. J.* **2019**, *25*, 1108.
[269] D. Kumar Gupta, M. H. Ali, A. Ali, P. Jain, M. K. Anwer, Z. Iqbal, M. A. Mirza, *J. Drug Targeting* **2022**, *30*, 131.

Arianna Grivet-Brancot is a Ph.D. candidate in Bioengineering and medical-surgical sciences at Politecnico di Torino and Università di Torino. She obtained her master degree in Biomedical Engineering from Politecnico di Torino in 2017. Before starting her Ph.D., she worked at Politecnico di Torino and National Institute of Research in the field of biomaterial development and characterization for the design of stimuli-responsive and drug delivery hydrogels.

Monica Boffito graduated cum laude in Biomedical Engineering in 2010 and obtained her Ph.D. in Biomedical Engineering in 2014 at Politecnico di Torino (Italy). She has documented experience in biomaterial design, characterization, and processing into 3D scaffolds or injectable hydrogels (stimuli-responsive and supramolecular hydrogels). After receiving her Ph.D., she worked at Politecnico di Torino, first as postdoc fellow, then as researcher with fixed-term contract, becoming a tenure-track researcher in 2019. She is the author of 31 publications in peer-reviewed journals, 6 book chapters, 2 editorials, and 2 patents. She has an h-index of 16 with around 800 citations (SCOPUS).

Gianluca Ciardellihas a master degree cum laude in Chemistry from the University of Pisa (Italy) and a Ph.D. in Natural Sciences from the Swiss Federal Institute of Technology of Zurich. He is currently full professor at Politecnico di Torino, Italy. He is coordinating a group carrying out research in the development of biomedical polymers and realization of scaffolds for tissue engineering, drug delivery in nanomedicine, experimental organ models. The Scopus database reports over 150 articles in peer-reviewed journals, 8 book chapters; 12 patents are cited by Espacenet. His h-index is 42 with more than 6000 citations (SCOPUS).